Southeastern Tanzania depositional environments, marine and terrestrial links, and exceptional microfossil preservation in the warm Turonian

Shannon J. Haynes[1,†], Kenneth G. MacLeod[1], Brian T. Huber[2], Sophie Warny[3], Alan J. Kaufman[4], Richard D. Pancost[5,6], Álvaro Jiménez Berrocoso[7], Maria Rose Petrizzo[8], David K. Watkins[9], and Iadviga Zhelezinskaia[4]

[1]*Department of Geological Sciences, University of Missouri, 101 Geology Building, Columbia, Missouri 65211, USA*
[2]*Department of Paleobiology, MRC 121, Smithsonian Museum of Natural History, Washington, DC 20013, USA*
[3]*Department of Geology and Geophysics & Museum of Natural Science, Louisiana State University, E235 Howe Russell, Baton Rouge, Louisiana 70820, USA*
[4]*Department of Geology and Earth System Science Interdisciplinary Center, University of Maryland, College Park, Maryland 20742-4211, USA*
[5]*Organic Geochemistry Unit, School of Chemistry, The Cabot Institute, University of Bristol, Cantock's Close BS8 1TS, UK*
[6]*Cabot Institute, University of Bristol, Bristol BS8 1UJ, UK*
[7]*Repsol Services Company, 2455 Technology Forest Boulevard, Building 5, The Woodlands, Texas 77381, USA*
[8]*Dipartimento di Scienze della Terra "Ardito Desio," Università degli Studi di Milano, via Mangiagalli 34, 20133 Milan, Italy*
[9]*Department of Earth and Atmospheric Sciences, University of Nebraska–Lincoln, Lincoln, Nebraska 68588-0340, USA*

ABSTRACT

Sediment cores from southeastern Tanzania contain exceptionally well-preserved calcareous and organic-walled microfossils in numerous samples spanning from the Aptian to the Miocene. The unusually high quality of preservation is commonly attributed to shallow burial and high clay content of the host sediments. However, such attributes apply to many deposits that are not characterized by exceptional preservation, and, thus, invoking only grain size and burial depth is clearly an incomplete explanation for the exceptional microfossil preservation. In an attempt to better characterize additional factors that were important in creating the Tanzanian microfossil lagerstätte, we integrated a wide range of paleontological, geochemical, and sedimentological observations to constrain the paleoenvironmental and early diagenetic conditions of a Turonian interval where exceptional preservation is common. Planktic microfossil assemblages suggest that open-ocean surface-water conditions prevailed at the site, but, despite excellent organic matter preservation, marine biomarkers are rare. The sediments are dominantly composed of terrigenous silts and clays and terrestrially derived organic matter. Paleontological and geochemical observations record a remarkably stable interval dominated by excellent preservation through the Lower–Middle Turonian. During the Middle–Upper Turonian, though, the preservation quality declines, and this is associated with notable shifts in foraminiferal assemblages, palynological species diversity, carbon and sulfur isotope compositions, and biomarker distributions. The integrated data suggest that an increase in subsurface microbial activity and associated changes in pore-water chemistry were important proximate variables that led to the decline in the quality of microfossil preservation up section within these shallowly buried, Turonian silty claystones from Tanzania.

INTRODUCTION

Hemipelagic mudstones from coastal Tanzania are renowned for the excellent preservation of the calcareous microfossils they contain, a characteristic that has facilitated a myriad of paleontological and paleoclimatological studies. Recent paleontological advances include recognition of remarkably diverse calcareous microfossil assemblages presented in detailed taxonomic papers on calcareous nannofossils as well as planktic and benthic foraminifera. These studies have resulted in the revision of phylogenetic histories and deeper insights into the paleoecology of calcareous microfossils (Lees, 2007; Bown et al., 2008, 2014; Wendler et al., 2011, 2013, 2016; Falzoni et al., 2013; Pearson and Coxall, 2014; Huber and Petrizzo, 2014; Haynes et al., 2015; Lees and Bown, 2016). For paleoclimatological studies, the exceptional preservation reduces uncertainty related to potential diagenetic overprinting of isotope compositions and biomarker distributions. In turn, this increases our confidence in arguments about greenhouse climates, including studies concluding that the cool tropics paradox was a preservational artifact (Pearson et al., 2001) and that the Turonian was effectively ice free (MacLeod et al., 2013).

The high quality of microfossil preservation has generally been attributed to the tests being buried at relatively shallow depths in clay-dominated sediments (e.g., Pearson et al., 2001; Bown et al., 2008, 2014; Dunkley Jones et al., 2009; Jiménez Berrocoso et al., 2010, 2012, 2015). However, there are many sites that preserve shallowly buried, fine-grained sediments that do not contain exceptionally well-preserved microfossils. Even within the Lindi region of Tanzania, preservation quality varies within facies and among sites that had almost identical burial histories and sediment compositions. For example, Santonian–middle Campanian (ca. 86–74 Ma) clay-rich rocks are well represented in recovered cores from Tanzania, but excellent preservation has not yet been found for this interval, even though both younger and older intervals do exhibit exceptional preservation (Jiménez Berrocoso et al., 2010, 2012, 2015). On much shorter time scales, specimens that are exceptionally well preserved often co-occur with those that are more poorly preserved

†sjh2c4@mail.missouri.edu

GSA Bulletin; doi: 10.1130/B31432.1; 14 figures; 2 tables; Data Repository item 2016305.

within washed residues of individual samples. Thus, clay-dominated sediments and shallow burial are incomplete explanations, even locally, for the taphonomic conditions that led to exceptional preservation in many intervals from the Aptian through the Miocene in Tanzania.

This integrative study presents Turonian (ca. 94–90 Ma) paleontological (foraminifera, calcareous nannoplankton, pollen, spores, and dinoflagellates), sedimentological, and geochemical (organic carbon isotopes, carbonate carbon and oxygen isotopes, sulfur isotopes, and biomarker distributions) data with the goal of characterizing the depositional and diagenetic environment associated with lagerstätte (i.e., exceptionally good) foraminiferal preservation. Better understanding of the depositional environment, including inferences about conditions in nearby terrestrial areas, will provide constraints for paleoclimatic interpretations of isotopic results and will help make generalizations concerning the taphonomic pathways that promote exceptional microfossil preservation.

METHODS

An integrative approach was taken to examine the Turonian marine depositional environments in southeastern Tanzania, with analyses focused on samples from Tanzania Drilling Project (TDP) Site 31 (10°1′49.80″S, 39°38′44.00″E), and augmented by additional observations reported for nearby Sites 22 (10°4′9.20″S, 39°37′9.50″E) and 36 (10°1′45.36″S, 39°38′12.42″E). Excellent microfossil preservation is present through most of the core recovered from Site 31, which is located 8 km southwest of Lindi (Figs. 1 and 2). Recovered material from Site 31 belongs to the Lindi Formation (Upper Albian to Coniacian; Jiménez Berrocoso et al., 2015) and spans the *Helvetoglobotruncana helvetica*, *Marginotruncana schneegansi*, and the lower *Dicarinella concavata* zones. Similar to all TDP sites that recovered Turonian material, Site 31 is dominated by laminated to thinly bedded mudstones with little evidence for bioturbation. Pyritized burrows have been documented throughout Site 31, but their abundance, which is based on qualitative observations, is described as rare or absent throughout most of the section (Wendler et al., 2016). Massive, fine-grained sandstones are a minor component of the lithology, and restricted occurrences of soft-sediment deformation are present (Fig. 3; Jiménez Berrocoso et al., 2012). Site 31 is particularly attractive for study of preservation because foraminiferal assemblages are well documented, species-specific isotopic patterns are well constrained by a large data set, preservation is excellent through most of the section, and depositional conditions appear to have been quite stable for long intervals (Jiménez Berrocoso et al., 2012, 2015; Wendler et al., 2013, 2016; Huber and Petrizzo, 2014; MacLeod et al., 2013; Huber et al., 2017). This site is also of interest because stratigraphic changes in preservation provide a natural taphonomic experiment. In contrast to the excellent microfossil preservation throughout most of the lower 86 m of the section, preservation declines markedly above 28 m depth (Fig. 4).

Data discussed here include published results on sedimentological descriptions, planktic and benthic foraminiferal distributions, carbon and oxygen isotopes of bulk carbonates, bulk organic carbon isotopes, carbon and oxygen isotopes derived from planktic and benthic foraminifera, high-resolution grain-size analyses, and calcareous nannofossil distributions (Jiménez Berrocoso et al., 2010, 2012, 2015; MacLeod et al., 2013; Huber and Petrizzo, 2014; Haynes et al., 2015; Wendler et al., 2016; Huber et al., 2017). New data on hydrocarbon biomarker compositions at Sites 22, 31, and 36, palynomorph assemblages at Sites 31 and 36, and sulfur abundance and isotope compositions at Site 31 are also reported and integrated to provide a detailed characterization of the Turonian succession.

Biomarkers

Extractions

Solvent extractions and analysis of lipid compositions on a gas chromatograph (GC) and gas chromatograph–mass spectrometer (GC-MS) were done at the University of Bristol following methods of van Dongen et al. (2006). To obtain organic carbon compounds from bulk sediments, ~4 g of material were finely powdered and then sequentially extracted (6×) using dichloromethane (DCM) and methanol (MeOH) mixtures in ratios of 1:0, 1:0, 1:1, 1:1, 0:1, and 0:1. Apolar and polar fractions were separated using flash column alumina chromatography with *n*-hexane:DCM (9:1) and DCM:MeOH (1:1) as eluents, respectively. Within 24 h of analysis, polar fractions were derivatized by adding 25 µL of *N*,*O*-bis(trimethylsilyl) triuoroacetamide (BSTFA, Sigma-Aldrich) and 25 µL of pyridine, followed by heating at 70 °C for 1 h.

Samples were analyzed using a Hewlett-Packard 5890 series II GC equipped with a flame ionization detector and a Phenomenex Zebron ZB-1 fused silica column (length = 60 m, inner diameter [ID] = 0.32 mm, film thickness [FT] = 0.1 µm). Hydrogen was used as the carrier gas. The temperature program ramped up from 70 °C to 130 °C at a rate of 20 °C/min, then from 130 °C to 300 °C at a rate of 4 °C/min. Temperature was then held constant at 300 °C for 25 min. The same temperature program was used

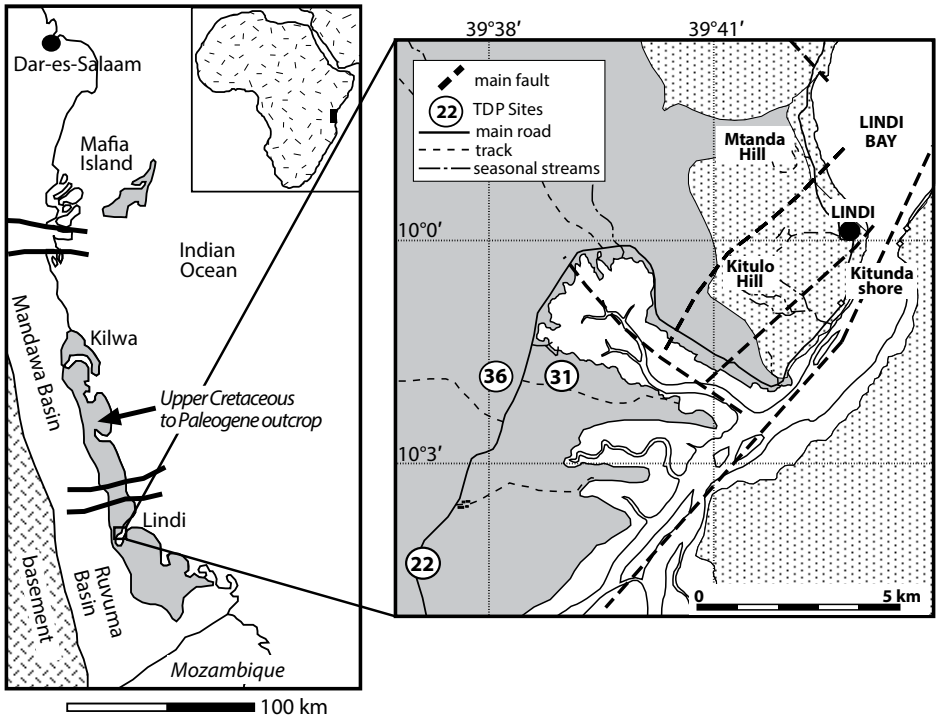

Figure 1. Map of study region in southeast Tanzania, modified from Jiménez Berrocoso et al. (2010). TDP—Tanzania Drilling Project.

for GC-MS, although helium was used as the carrier gas. The GC-MS was a Finnigan Trace GC-MS fitted with a 50 m Agilent HP-1 fused silica column (ID = 0.32 mm, FT = 0.17 µm).

Palynology

In total, 24 samples were processed for palynological evaluation at the Center for Excellence in Palynology (CENEX) at Louisiana State University, Baton Rouge, Louisiana (Tables DR1 and DR2[1]). All samples were dried, weighed, and spiked with a known quantity of *Lycopodium* spores prior to processing to allow for concentration computation. Samples were then treated with HCl and HF to remove carbonates and silicates. To isolate the palynomorphs from the remaining organic fraction, the residues underwent heavy liquid separation and were sieved through a 10 µm mesh (Brown, 2008). The final residues were mounted on microscope slides with glycerine jelly. A minimum of 300 palynomorphs were counted per sample. Palynomorph concentrations were calculated as follows: $cc = (P_c \times L_t \times T)/(L_c \times W)$, where cc = concentration per gram of dried sediment, P_c = the number of palynomorphs counted, L_t = the number of *Lycopodium* spores per tablet, T = the total number of *Lycopodium* tablets added per sample, L_c = the number of *Lycopodium* spores counted, and W = the weight of dried sediment.

Sulfur Abundance and Isotope Compositions

Total sulfur in bulk powders was analyzed initially by elemental analysis combustion techniques, but low overall sulfur contents in the core required that most samples be extracted using a chemical reduction method that targeted elemental and pyrite-bound sulfur. In this technique, 0.5–3 g aliquots of powdered material were weighed and reacted with 0.5 *M* HCl and 20 mL of a chromium reducing solution (Canfield et al., 1986) for 3.5 hours, producing gaseous H_2S that was carried in a stream of N_2 gas and bubbled through 20 mL of a 0.026 *M* $AgNO_3$ plus 0.167 *M* HNO_3^- capture solution to precipitate S as Ag_2S. The black precipitates were aged in the dark for a week and then washed with 15 mL of 1 *M* NH_4OH and ultrapure Milli-Q water, dried overnight in an 80 °C oven, and then weighed. The purified Ag_2S yields were used to calculate the pyrite abundance in the bulk samples.

[1]GSA Data Repository item 2016305, supplementary tables including relevant geochemical and biostratigraphic data, is available at http://www.geosociety.org/pubs/ft2016.htm or by request to editing@geosociety.org.

The pyrite sulfur isotope abundances were measured by combustion of ~100 mg of Ag_2S or 1–5 mg of bulk powder to SO_2 with a EuroVector elemental analyzer. Samples were combusted in a 1030 °C furnace. SO_2 was separated from other gases with a 0.8 m polytetrafluoroethylene (PTFE) GC column packed with Porapak 50–80 mesh heated to 115 °C. Sulfur isotopes were measured on an Elementar Isoprime isotope ratio mass spectrometer (IRMS) operated in continuous-flow mode using He as the carrier gas. Sulfur isotope ratios (m/z 66/64) were determined relative to known values for a reference gas and are expressed in delta notation (δ) as per mil (‰) deviations from the Vienna Canyon Diablo Troilite (VCDT) standard. Two NBS-127 barite standards and two International Atomic Energy Agency (IAEA) NZ1 silver sulfide standards were measured between every 10 samples for drift and offset corrections. Uncertainties for each analytical session based on these standard analyses were determined to be better than 0.3‰.

RESULTS AND INFERENCES

Here, we present new data and summarize published observations; each subsection describes the general implications for the paleontological, geochemical, and sedimentological observations individually. The subsequent discussion section integrates the combined observations to provide a descriptive model of Turonian deposition in southeast Tanzania, with particular emphasis on aspects of the depositional and diagenetic environment that resulted in the microfossil lagerstätte.

Preservation

The excellent preservation of foraminifera and other calcareous microfossils at TDP Site 31 is well documented (e.g., Wendler et al., 2011, 2013, 2016; MacLeod et al., 2013; Wendler and Bown, 2013; Huber and Petrizzo, 2014). Palynomorphs extracted from these sections are some of the best preserved from Late Cretaceous strata worldwide, and they far surpass preservation in equivalent strata from Colombia and Canada (e.g., Sweet and McIntyre, 1988; Garzon et al., 2012; Akyuz et al., 2015). High-magnification scanning electron microscope images and multifocus light microscope images of calcareous and organic-walled microfossils illustrate the remarkable preservation of wall microstructure with no evidence of recrystallization or overgrowth of diagenetic calcite down to a submicron scale and no oxidation of the organic fossils (Fig. 2).

This level of preservation is typical of specimens throughout the lower 86 m of Site 31 (cores 19–64; Fig. 4), but not all specimens are so well preserved. Specimens infilled with diagenetic calcite are present between 95 and 105 m, 75 and 80 m, and 30 and 40 m (Wendler et al., 2016), and evidence of dissolution in some specimens becomes more common above ~54 m. Preservation quality dramatically declines above ~28 m, between the top of core 19 at 28.1 m and the bottom of core 18 at 27.3 m, with specimens being largely infilled and commonly recrystallized (Fig. 4).

Paleontological Observations

Foraminifera

The planktic foraminiferal assemblage suggests a fully marine and mostly oligotrophic environment, given its high diversity (>25 taxa; Huber et al., 2017) and the fact that many of the species present are common in correlative open-ocean, organic carbon-poor, pelagic chalks (e.g., Petrizzo, 2000, 2001, 2003). Planktic foraminifera are relatively abundant in the early–middle Turonian interval (cores 19–64; Figs. 4 and 5A), and foraminiferal assemblages consistently include mature specimens of key marker species, which are commonly used to subdivide the standard zonal schemes applied to low-latitude deep-sea sequences (Fig. 5A; Jiménez Berrocoso et al., 2010, 2012, 2015; Huber et al., 2017). However, the Tanzanian assemblages differ from those typically found in pelagic carbonate sediments in that there are consistent occurrences of small morphotypes, which either represent ecophenotypes (of several species) or which should be described as new species. For example, the species *Praeglobotruncana stephani* only occurs as diminutive ("dwarfed") morphotypes above 45 m (core 27). Restriction of these small morphotypes to shallower-water settings is suggested by their absence from coeval deep-sea samples, but confirmation of this requires their identification in similar deposits elsewhere. Alternatively, the presence of small morphotypes may simply reflect the high quality of preservation as more fragile tests might be lost elsewhere due to dissolution and fragmentation.

The Turonian planktic assemblages show very little change throughout the *Helvetoglobotruncana helvetica* zone, but there are two shifts in species populations in the upper half of the sequence recovered at Site 31. One shift occurs between 45 and 41 m (between cores 27 and 25) across the level where *H. helvetica* (Bolli, 1945) disappears. The second shift occurs at ~28 m (between cores 19 and 18) within the *Marginotruncana schneegansi*

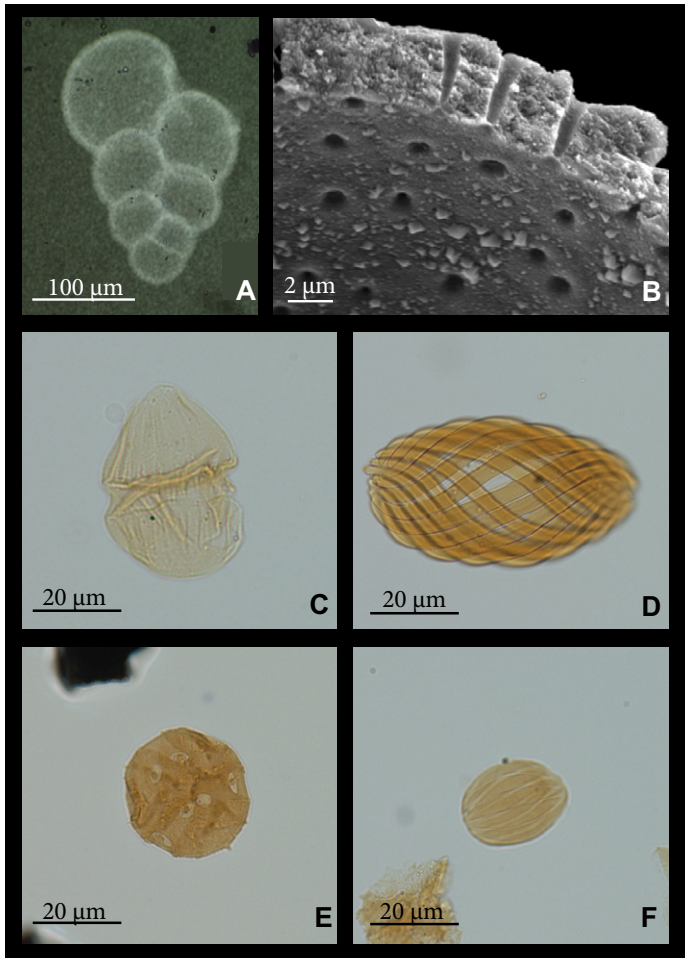

Figure 2. Examples of exceptionally well-preserved material from Tanzania Drilling Project (TDP) Site 31. (A) X-ray photomicrograph of *Planoheterohelix paraglobulosa* from sample TDP 31–44–1, 22–42 cm, showing the absence of infilling in well-preserved specimens. (B) X-ray photomicrograph of *Planoheterohelix globulosa* from sample TDP 31–25–1, 77–81 cm, close-up scanning electron microscope (SEM) image of test wall microstructure showing little to no recrystallization of test wall. (C–F) Light photomicrographs all at identical scale: (C) Example of a common dinoflagellate cyst, *Dinogymnium* sp.; (D,F) examples from the *Ephedripites* group; and (E) angiosperm pollen grain, *Hexaporotricolpites* sp.

zone (Fig. 5B). The lower shift marks an interval of foraminiferal turnover. Three species (*Helvetoglobotruncana praehelvetica* [Trujillo] 1960, *Dicarinella hagni* [Scheibnerová] 1962, and *Whiteinella aprica* [Loeblich and Tappan] 1961) have highest occurrences in the same sample as the highest occurrence of *H. helvetica* at ~42 m (between cores 26 and 25; Fig. 5B). This boundary interval, marked by the extinction of *H. helvetica*, also correlates with a decrease in size of specimens belonging to the species *Praeglobotruncana stephani* (Gandolfi, 1942). Just above and below the extinction level

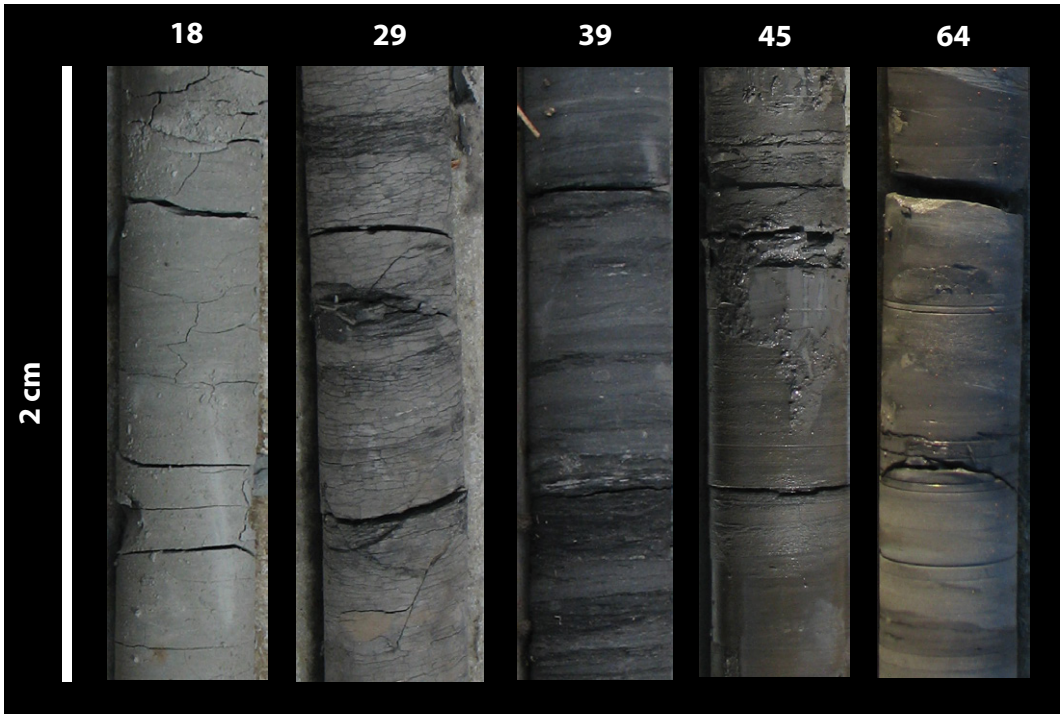

Figure 3. Photos of drilled cores from Tanzania Drilling Project (TDP) Site 31; numbers above the images indicate the core numbers. Core photos were previously published in Wendler et al. (2016).

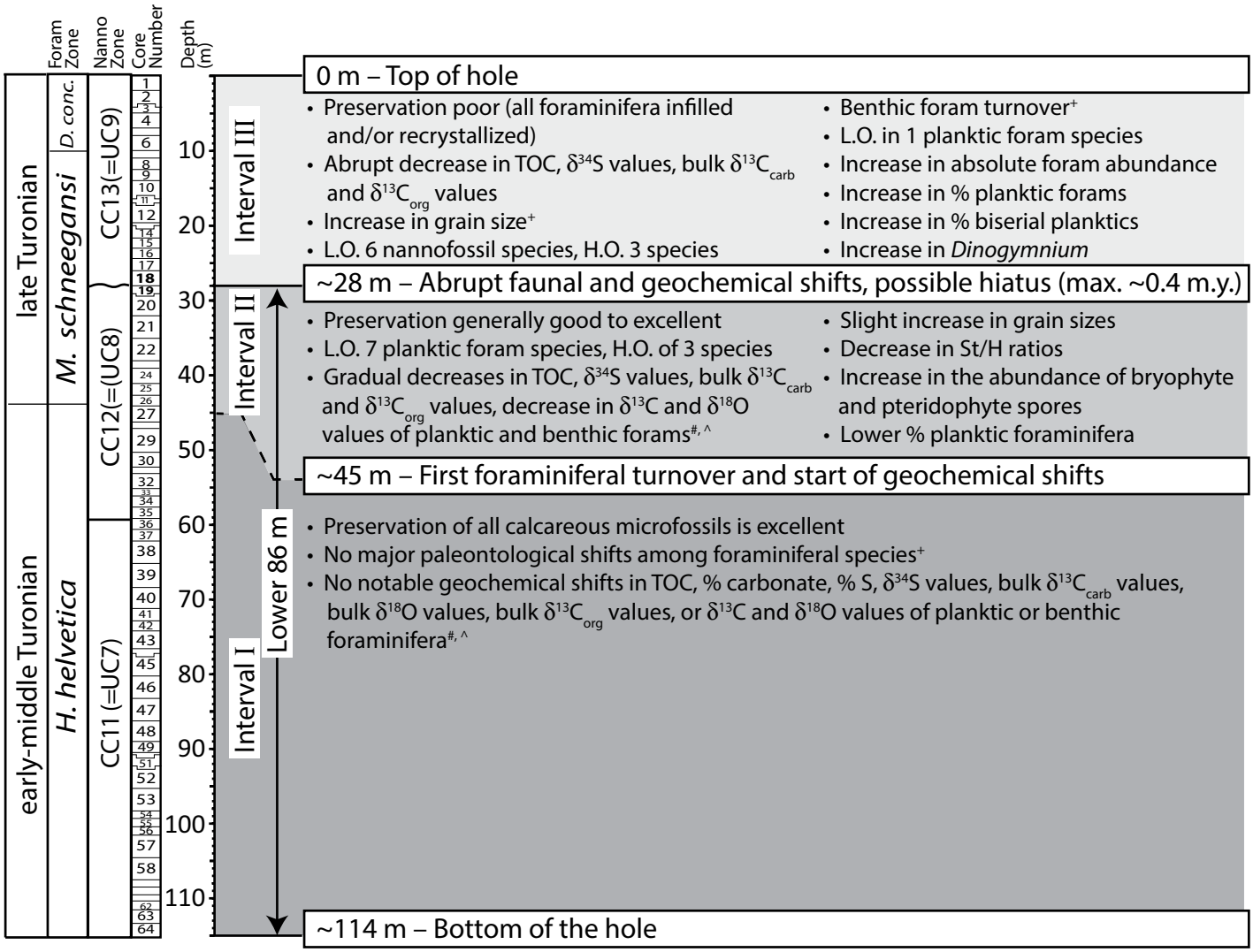

Figure 4. Summary of major paleobiological and geochemical changes at Tanzania Drilling Project (TDP) Site 31. Lower dark-gray panel includes changes between the bottom of the hole up to ~45 m, middle-gray panel includes changes across the interval between 45 m and 28 m, and the top light-gray panel includes changes occurring at 28 m. Abbreviations are as follows: foram(s)—foraminifera, TOC—total organic carbon content, L.O.—lowest occurrence, H.O.—highest occurrence, nanno—calcareous nannofossils, and St/H—diasterene/hopane ratios. Plus (+) indicates changes in benthic foraminiferal assemblages from Wendler et al. (2016); pound symbol (#) indicates foraminiferal $\delta^{13}C$ and $\delta^{18}O$ data from MacLeod et al. (2013); and caret (^) indicates bulk carbonate $\delta^{13}C$ and $\delta^{18}O$ data as well as % carbonate and TOC data from Jiménez Berrocoso et al. (2012). Abbreviations are as follows: *H.—Helvetoglobotruncana*, *M.—Marginotruncana*, *D.—Dicarinella*, CC—Cretaceous Coccolith zonation of Perch-Nielsen (1985), and UC—Upper Cretaceous zonation.

(i.e., between 45 and 41 m; Fig. 5B), we find the lowest occurrences of seven planktic species, including four species of *Marginotruncana* (*Marginotruncana angusticarenata* [Gandolfi] 1942, *Marginotruncana caronae*, Peryt 1980, *Marginotruncana pseudolinneiana*, Pessagno 1967, and *Marginotruncana sinuosa*, Porthault 1970) and three species of biserial planktic foraminifera (*Laeviheterohelix reniformis* [Marie] 1941, *Planoheterohelix reussi* [Cushman] 1938, and *Planoheterohelix praenuttalli* Haynes et al. 2015 [Haynes et al., 2015]).

The upper shift at ~28 m (Fig. 5B) does not coincide with any range terminations among foraminifera and correlates with the lowest occurrence of only one planktic species, *Marginotruncana undulata* (Lehmann) 1963. This level is notable, however, because above 28 m, there is a dramatic increase in the total number of foraminifera, as well as an increase in the relative abundance of biserial planktic foraminifera (Figs. 5A and 5B). The volume of sediment processed for each foraminiferal sample was ~1500 cm^3. On average, each sample below 28 m contained ~3500 foraminifera (= ~2 foraminifera/cm^3), whereas above 28 m, each sample contained ~24,000 (= ~16 foraminifera/cm^3). The relative abundance of biserials increased from ~10% to ~50% of the planktic assemblage, or ~4% to 35% of the total foraminiferal assemblage, over the same interval (Fig. 5A). The abrupt increase in percentage of biserials is not an artifact of diminished numbers of other planktic foraminifera because all foraminiferal taxa (planktic and benthic) are more abundant in the upper interval of Site 31. In other words, absolute abun-

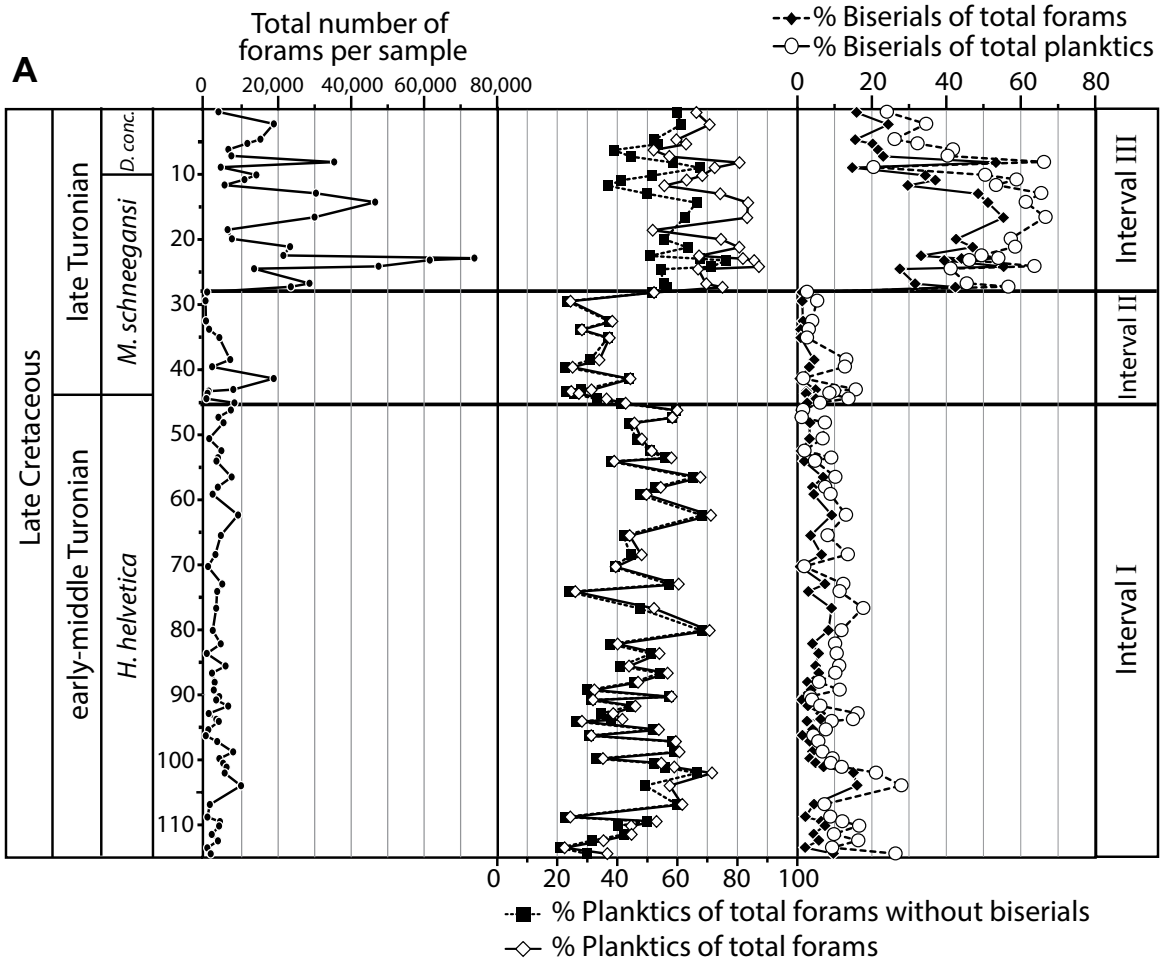

Figure 5 (*on this and following page*). Foraminiferal distributions at Tanzania Drilling Project (TDP) Site 31. (A) General abundance of foraminifera; all data referring to abundance of benthic foraminifera are from Wendler et al. (2016). (B) Ranges of common trochospiral planktic species, including small or "dwarfed" forms and "affinis" forms that are morphologically transitional from ancestral taxa. For full biostratigraphy of non-biserial planktic foraminifera for TDP Site 31, refer to Huber et al. (2017). Abbreviations are as follows: *A.—Archaeoglobigerina*, *D.—Dicarinella*, *F.—Falsotruncana*, *H.—Helvetoglobotruncana*, *M.—Marginotruncana*, and *W.—Whiteinella*, CC—Cretaceous Coccolith zonation of Perch-Nielsen (1985), and UC—Upper Cretaceous zonation.

dance of biserial taxa increases by 60×, while other taxa increase in abundance by 4× across the 28 m horizon (Fig. 5A).

Differences in the relative proportions among and between planktic and benthic taxa in stratigraphically ordered fossil assemblages can reflect variations in one or more paleoenvironmental factors, including paleodepth, water chemistry, nutrient abundances, surface-water productivity, and the depth of the lysocline (Gibson, 1989). Although the relative abundance of planktic foraminifera varies throughout the Turonian at Site 31, we argue the shifts at ~42 m (between 45 and 41 m) and 28 m are the ones most likely to indicate factors of paleoenvironmental significance. Based on planktic percentage values, where planktic percentage = (number of planktics/total number of foraminifera) × 100, the record from the bottom of the borehole to the onset of the planktic foraminiferal turnover at 45 m yields planktic percentages that average 47% (±13%, 1 standard deviation [SD]); between 45 m and 28 m, the planktic percentages decrease slightly to 36% (±10%, 1 SD); and in the upper interval, with poor preservation (above 28 m), the planktic percentages increase to 72% (±11%, 1 SD; Fig. 5A). Based on comparison with data sets for modern foraminiferal distributions (Gibson, 1989), the planktic percentages at Site 31 are consistent with deposition at outer-shelf to upper-slope paleodepths (Jiménez Berrocoso et al., 2012, 2015; Wendler et al., 2016). The shift to lower abundances of planktic foraminifera in the middle interval (between 45 m and 28 m; Fig. 4) could have been caused by a drop in relative sea level, a decrease in planktic foraminiferal productivity, or an increase in benthic foraminiferal productivity, whereas the shift to higher planktic abundances in the upper interval could represent an increase in relative sea level, a major increase in planktic foraminiferal productivity, or a major decrease in benthic foraminiferal productivity.

Benthic foraminifera at Site 31 are diverse and include taxa that are typical of deposition at upper-bathyal to outer-neritic paleodepths (Jiménez Berrocoso et al., 2012; Wendler et al., 2011, 2013, 2016). Species of benthic foraminifera such as *Tappanina lacinosa* that typically indicate low-oxygen conditions are rare to absent throughout the section, suggesting consistently oxygenated bottom waters (see fig. 5 *in* Wendler

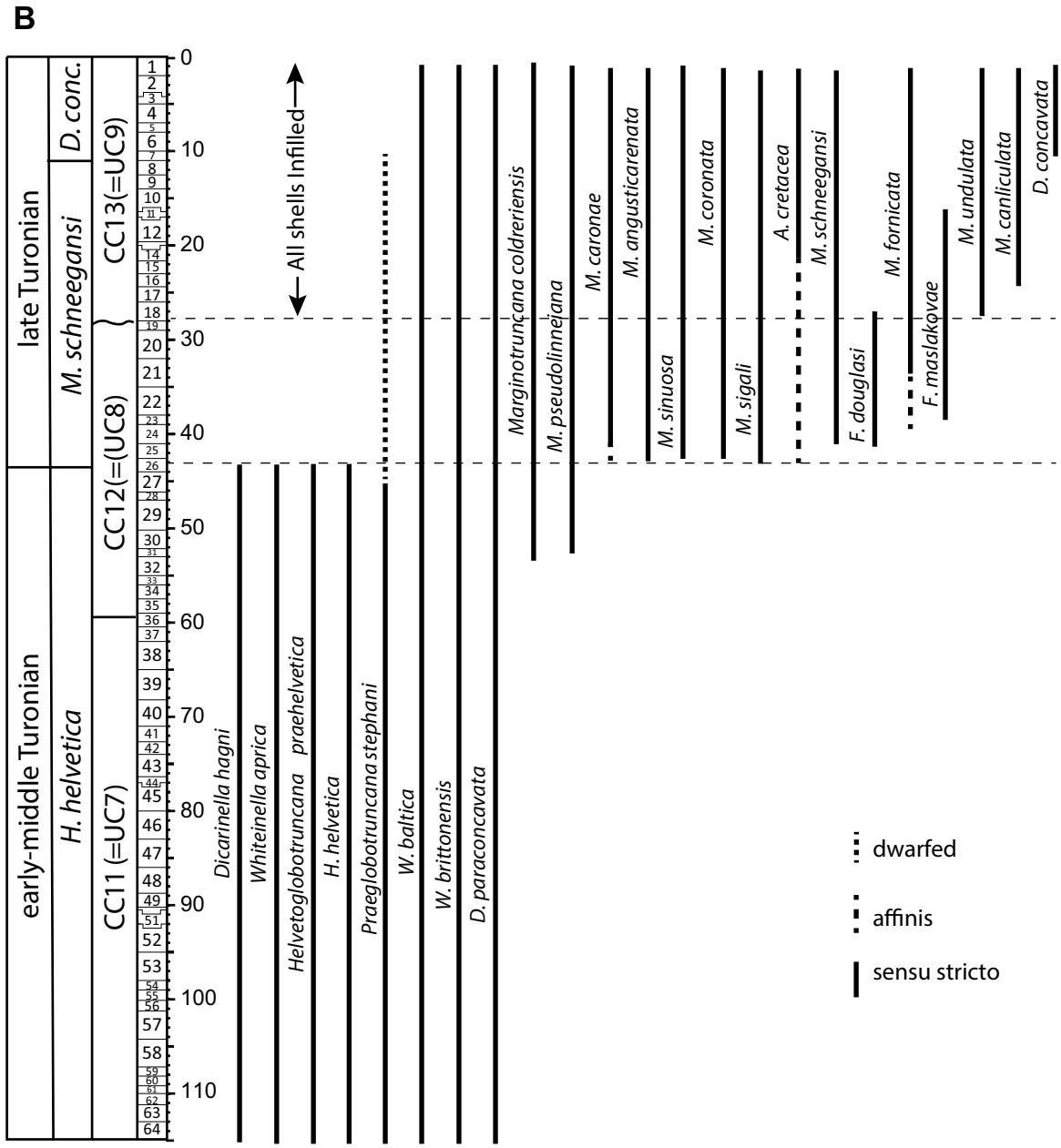

Figure 5 (*continued*).

et al., 2016). According to Wendler et al. (2016), the benthic foraminiferal population below 45 m is largely dominated by species belonging to the genera *Ammodiscus*, *Berthelina*, *Ceratobulimina*, *Colomia*, *Epistomina*, *Glomospira*, and *Lingulogavelinella*; above 28 m, it is largely dominated by species belonging to the genera *Allomorphina*, *Dentalina*, *Dorothia*, *Frondicularia*, *Gaudryina*, *Gavelinella*, *Gyroidinoides*, *Nodosaria*, *Pleurostomella*, *Quadrimorphina*, *Ramulina*, *Reussella*, *Spiroplectammina*, and *Stensioeina*. A decrease in the assemblage typical of older samples occurs at ~45 m and is mirrored by a gradual replacement of those more prominent in the upper portion of the section, with an abrupt increase in the younger assemblage at 28 m. Wendler et al. (2016) primarily attributed the shifts at 45 m and 28 m to drops in sea level, but changes in nutrient availability (causing increased surface productivity) and physicochemical conditions of the bottom and surface waters could also explain the shifts.

Calcareous Nannofossils

The detailed biostratigraphy for the calcareous nannofossils from the Turonian TDP sites is presented in Huber et al. (2017). A summary of their results that pertain to Site 31 is presented here. Biostratigraphic assignments follow the Cretaceous Coccolith (CC) zonation of Perch-Nielsen (1985) and the Upper Cretaceous (UC) zonation of Burnett (1998).

Calcareous nannofossils are well preserved and generally abundant in TDP Site 31 material, with only a small number of samples exhibiting moderate preservation. For the most part, the composition and structure of the nannofossil assemblage are comparable with coeval assemblages from open-ocean sites with high diversity. Samples from cores 36–64 (59–115 m) contain nannofossil assemblages that include *Quadrum*

gartnerii, *Eprolithus moratus*, and *Chiastozygus spissus*, indicating Lower Turonian calcareous nannofossil zone CC11 (= UC7; Fig. 6). The presence of *E. moratus* in the basal sample indicates that the lowermost Turonian is not represented in the recovered interval. Samples from cores 35–19 (~28–58 m) are characterized by nannofossils that include *Eiffellithus eximius* (sensu Verbeek, 1977), but lack *Marthasterites furcatus*, indicating zone CC12 (= UC8) of the uppermost Lower to lower Upper Turonian. Nannofossil assemblages through this interval generally exhibit normal, open-ocean character and structure.

A significant turnover of nannofossil species occurs at ~28 m (between cores 18 and 19; Fig. 6). Core 19 contains the last appearances of *Eprolithus moratus*, *Helicolithus turonicus*, and *Liliasterites atlanticus*, whereas core 18 includes the first appearances for *Lithastrinus septenarius*, *Marthasterites furcatus*, *Reinhardtites biperforatus*, and *Eiffellithus eximius* (s.s.). The termination of the stratigraphic ranges in core 19, and the co-occurrence of the first appearances in core 18 suggest that there is a hiatus between cores 19 and 18. Current calibration (Ogg and Gradstein, 2015) of the lowest occurrences of *R. biperforatus* and *M. furcatus* indicates that the missing time is ~0.4 m.y., but the quantitative biostratigraphy of Corbett et al. (2014) shows that these first appearance events are closely spaced in the late Turonian, and there are no corresponding range terminations among planktic foraminifera. Thus, the estimate of ~0.4 m.y. is considered to be a maximum duration for the hiatus.

Samples from 28 m to the top of the hole (cores 1–18) contain *M. furcatus* and other species typical of Upper Turonian zone CC13 (= UC9; Fig. 6). Diversity is generally high, and the structure of the assemblages suggests a continuation of open-ocean surface-water conditions. The rare occurrence of forms transitional to *Micula cubiformis* between ~5 and 8 m and the absence of *Micula staurophora*, which is used to denote the base of zone CC14 and is a proxy for the Turonian-Coniacian boundary, indicate that the samples were deposited close to, but still below, the Coniacian Stage.

Palynomorphs

The palynological assemblage is dominated by terrestrial taxa that preferred warm, arid environments. Approximately 90% of the

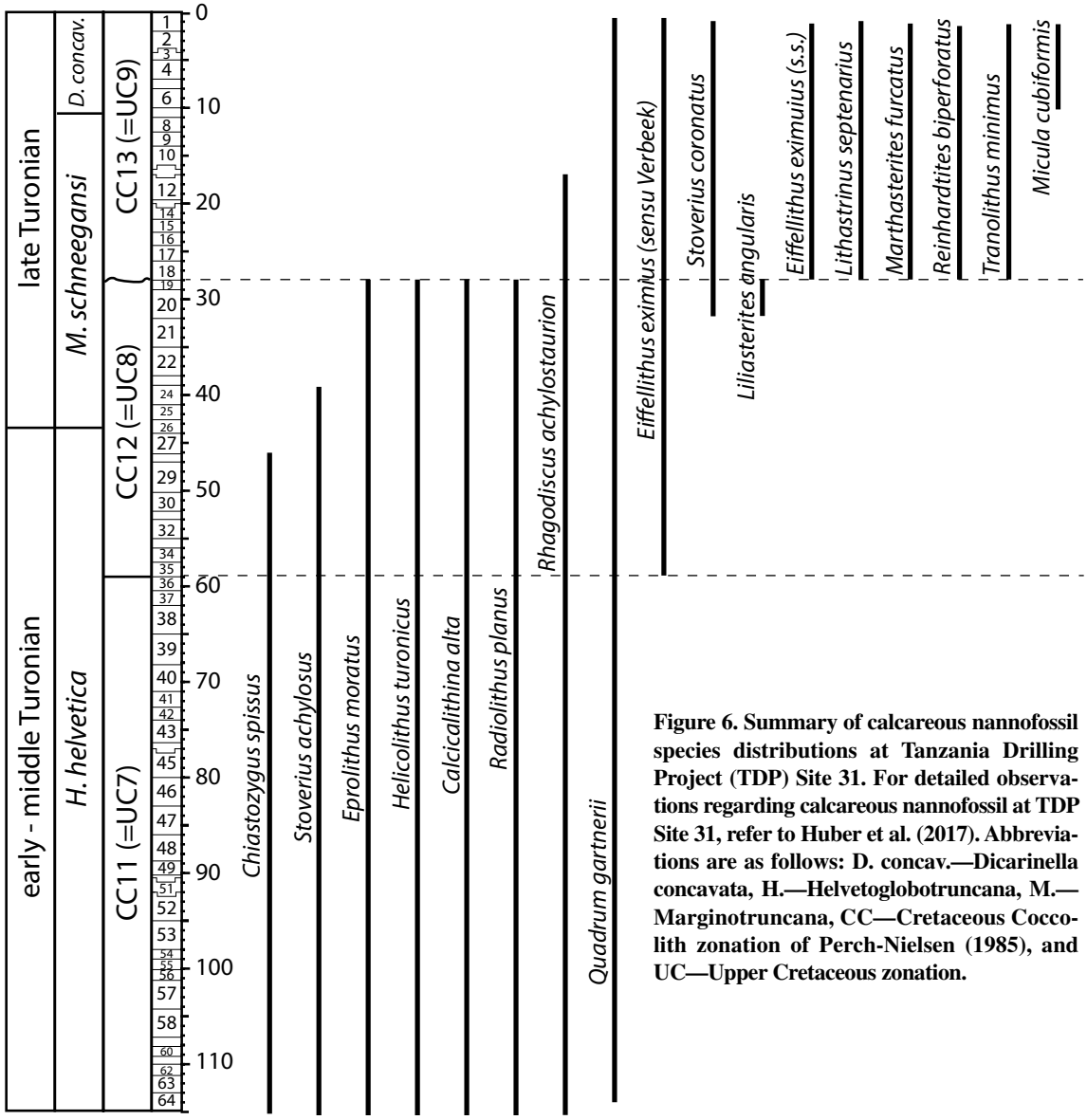

Figure 6. Summary of calcareous nannofossil species distributions at Tanzania Drilling Project (TDP) Site 31. For detailed observations regarding calcareous nannofossil at TDP Site 31, refer to Huber et al. (2017). Abbreviations are as follows: D. concav.—Dicarinella concavata, H.—Helvetoglobotruncana, M.—Marginotruncana, CC—Cretaceous Coccolith zonation of Perch-Nielsen (1985), and UC—Upper Cretaceous zonation.

assemblage is composed of spores and pollen from land plants and is strongly dominated by gymnosperms (Figs. 7A and 7B). The most common genera are *Classopollis*, *Ephedripites*, and *Exesipollenites* (Fig. 7B). The high relative abundance of terrestrial palynomorphs indicates that continental sources dominated the organic microfossil budget, with only minor contributions from marine dinoflagellates.

The terrestrially derived pollen and spores present in the sediments provide a means of characterizing contemporary environmental conditions on the nearby continent. *Classopollis*, possibly a member of the family Cheirolepidiaceae (Srivastava, 1976; Kürschner et al., 2013), is a pollen grain produced by an extinct conifer that lived in coastal regions. It has been proposed to be indicative of warm, dry conditions and seemed to favor well-drained soils of upland slopes and of lowlands (Srivastava, 1976). *Ephedripites* has also been suggested to be an indicator of aridity (Schrank, 2010), based on a presumed association with *Ephedra*, a prominent member of the floral groups living in arid to semiarid regions of the southwestern United States (Price, 1996). *Exesipollenites* has been proposed to derive from an extinct conifer that has been associated with arid climates (Li et al., 2015), and its abundance increases at ~50 m.

Arid conditions throughout the early and middle Turonian are also supported by the rarity of bryophytes and pteridophytes throughout the *Helvetoglobotruncana helvetica* zone at Site 31 (Fig. 7B). Because their reproduction is dependent on the presence of standing water, at least seasonally, the presence of these types of spores is usually indicative of humid conditions (Meyer, 1995). Interestingly, there is an increase in the abundance of bryophyte and pteridophyte spores above 45 m (Fig. 7B). Samples from this upper interval all continue to contain indicators of aridity, but the increase in bryophytes and pteridophytes suggests a regional increase in humidity during the late Turonian. Indicators of aridity correlated with plants dependent on wet events for reproduction may indicate an increase in episodic and/or intense precipitation and runoff in the late Turonian similar to what has been inferred for Tanzanian sediments deposited during warm Eocene intervals (Handley et al., 2012).

The marine palynomorphs that are present provide few constraints on paleoenvironmental

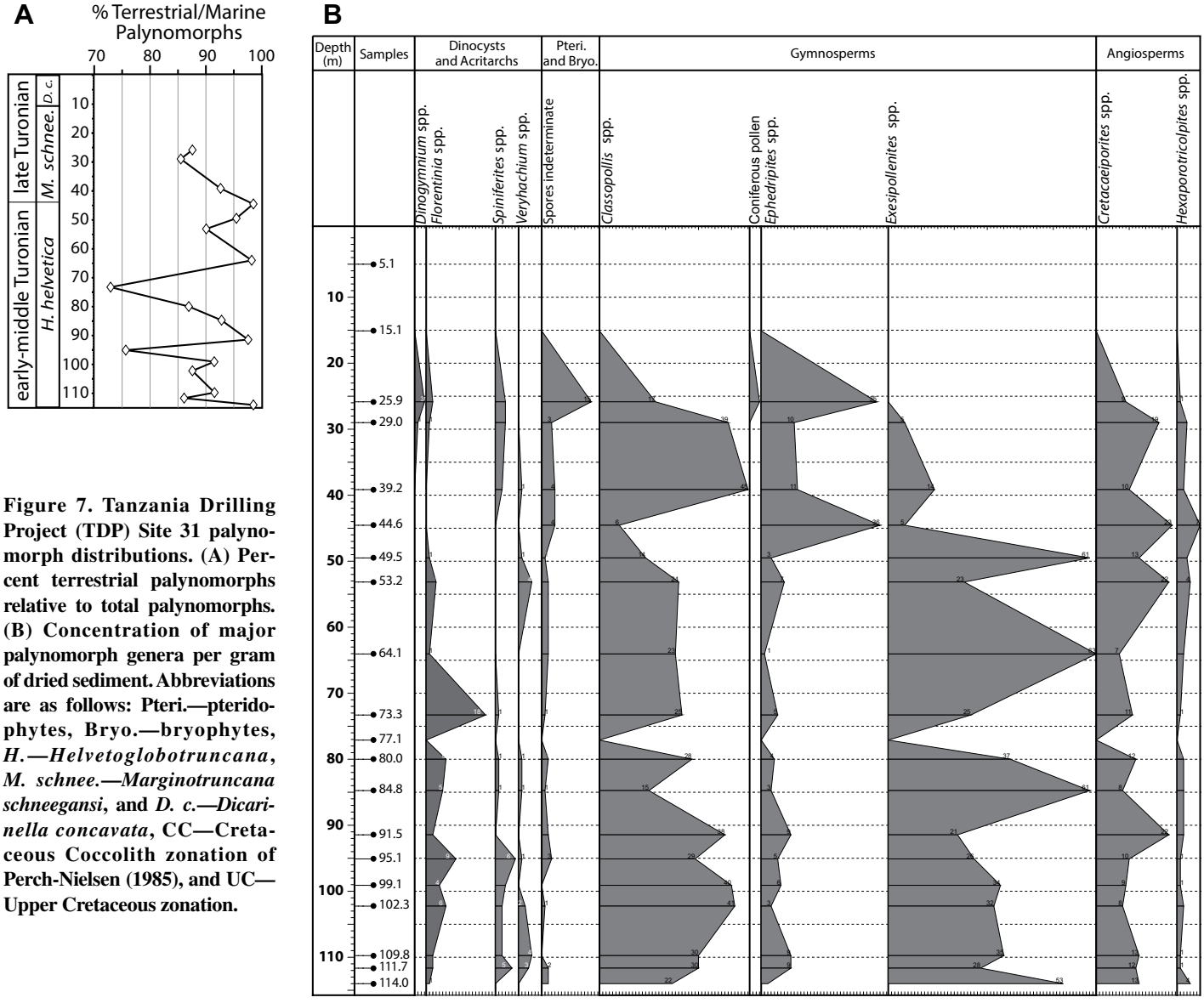

Figure 7. Tanzania Drilling Project (TDP) Site 31 palynomorph distributions. (A) Percent terrestrial palynomorphs relative to total palynomorphs. (B) Concentration of major palynomorph genera per gram of dried sediment. Abbreviations are as follows: Pteri.—pteridophytes, Bryo.—bryophytes, *H.*—*Helvetoglobotruncana*, *M. schnee.*—*Marginotruncana schneegansi*, and *D. c.*—*Dicarinella concavata*, CC—Cretaceous Coccolith zonation of Perch-Nielsen (1985), and UC—Upper Cretaceous zonation.

interpretations. Throughout Site 31, several prominent genera of marine dinoflagellate cysts and acritarchs are present, including *Florentinia*, *Spiniferites*, and *Veryhachium* (Fig. 7B). *Spiniferites* has been documented over a broad range of conditions, ranging from littoral to open-marine environments; little is known about the environmental preferences of either *Florentinia* or *Veryhachium*. Dinoflagellates are relatively common in samples from 95.1 m and from 73.3 m (Fig. 7B), but as sampling resolution is low, it is unclear whether occurrences at these levels reflect episodic variability within the lower portion of the section or sampling biases. A third increase in the relative abundance of marine taxa occurs above ~34 m (between cores 20 and 24; Fig. 7B). Unlike the two older intervals (at 95.1 m and 73.3 m), these younger samples include specimens of *Dinogymnium* (from samples at 25.9 m and 29.0 m; Fig. 7B), a taxon that is associated with estuarine settings, the inner shelf, or coastal waters (Garzon et al., 2012).

Geochemical Observations

Taking into consideration the marked paleontological and taphonomic transitions recorded at 28 m (between cores 18 and 19) and 45 m (between cores 26 and 27) at Site 31, the bulk geochemical data are binned into intervals I, II, and III, representing samples from below, between, and above these levels, respectively (Figs. 4 and 8). Average values for the abundance and isotopic composition of carbonate ($\delta^{13}C_{carb}$ and $\delta^{18}O_{carb}$), organic carbon ($\delta^{13}C_{org}$), and elemental and pyrite-bound sulfur ($\delta^{34}S_{TS}$ and $\delta^{34}S_{pyr}$) are presented in Table 1 (complete table of sulfur isotope and abundance data is given in Supplementary Table DR3 [see footnote 1]).

Bulk Carbonate, Organic Carbon, and Sulfur Abundances and Isotope Compositions

The abundance of carbonate in bulk samples from TDP Site 31 ranges from ~5% to 25%, and, on average, samples with the highest abundances are from the upper interval (III). Total organic carbon (TOC) content varies little within the lower 60 m of interval I (avg. I = 1.10%), but then it declines up section at the top of interval I and through interval II (avg. II = 0.84%), and then dramatically drops in interval III (avg. III = 0.26%; Fig. 8; Table 1). Coincident with the overall trend in TOC, bulk $\delta^{13}C_{carb}$, $\delta^{18}O_{carb}$, and $\delta^{13}C_{org}$ values decrease, especially the carbon isotope compositions (Fig. 8; Table 1).

It is important to note that none of the shifts in $\delta^{13}C_{carb}$ and $\delta^{13}C_{org}$ values throughout the section appears to be stratigraphically consistent and of comparable magnitude to those described for pelagic sequences such as the English Chalk (Jarvis et al., 2006, 2011). The Navigation Event originally described by Jarvis et al. (2006) could be stratigraphically correlated with a decrease in bulk $\delta^{13}C_{carb}$ and $\delta^{13}C_{org}$ values in interval III (Wendler et al., 2016; Fig. 8). However, the magnitude of the $\delta^{13}C_{carb}$ excursion at TDP Site 31 is almost 10× larger than previously observed (decreases by ~4‰ at TDP 31 [Fig. 8] vs.

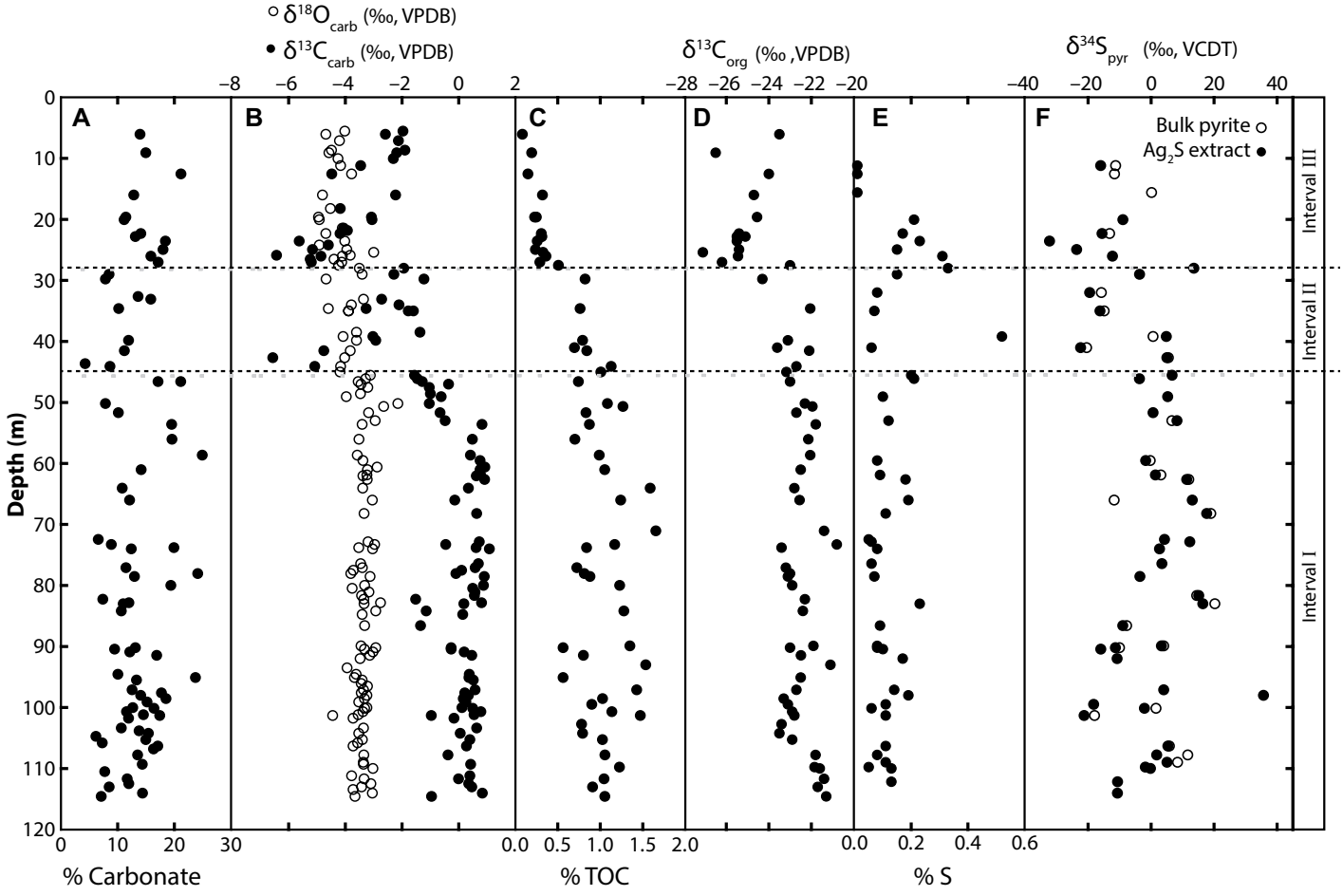

Figure 8. Depth profiles of bulk geochemical data for Tanzania Drilling Project (TDP) Site 31. TOC—total organic carbon; VPDB—Vienna Peedee belemnite; VCDT—Vienna Canyon Diablo Troilite.

TABLE 1. SUMMARY OF TANZANIAN DRILLING PROJECT (TDP) SITE 31 BULK CARBONATE, ORGANIC CARBON, AND SULFUR ABUNDANCES AND ISOTOPIC COMPOSITIONS

	Unit III (0–28 m)	Unit II (28–45 m)	Unit I (45–115 m)
% carbonate	16.60 ± 5.64	10.35 ± 3.45	13.72 ± 5.58
% TOC	0.27 ± 0.10	0.84 ± 0.15	1.09 ± 0.35
% S	0.14 ± 0.12	0.20 ± 0.19	0.12 ± 0.05
$\delta^{13}C_{carb}$ (‰)	–4.30 ± 2.39	–3.99 ± 3.05	–0.80 ± 2.10
$\delta^{18}O_{carb}$ (‰)	–4.29 ± 0.45	–3.85 ± 0.53	–3.48 ± 0.51
$\delta^{13}C_{org}$ (‰)	–25.12 ± 1.17	–22.98 ± 0.88	–22.43 ± 0.70
$\delta^{34}S_{TS}$ (‰)	–8.95 ± 6.14	–9.00 ± 11.34	3.69 ± 11.07
$\delta^{34}S_{pyr}$ (‰)	–18.11 ± 8.48	–5.47 ± 14.03	1.55 ± 11.47

Note: Average values are reported followed by ±1 standard deviation. TOC—total organic carbon; TS—total elemental sulfur; pyr—pyrite-bound sulfur.

the 0.4‰ decrease in the English Chalk [Jarvis et al., 2006]).

The sulfur abundance in all samples from Site 31 is remarkably low for fine-grained marine sediments. Although the highest sulfur concentrations are recorded in several samples from interval III, there is no statistical difference in the sulfur contents among the three intervals (Fig. 8). While the sulfur isotopic compositions of samples throughout the recovered section are highly variable (ranging from –30‰ to +35‰), there is a general up-section increase in $\delta^{34}S$ values, with maximum values at ~60 m (Fig. 8). Above this level, $\delta^{34}S$ values generally decline through the top of interval I and through intervals II and III. Due to the large amount of scatter in the $\delta^{34}S$ data, a Welch *t*-test (assumes normal distribution and unequal variances between the two populations) was preformed and shows that the average values in interval I are significantly different (p-value = 0.0113, two-tailed test) than those in the overlying intervals (i.e., II and III combined). A Mann-Whitney *U*-test confirms this conclusion by finding a significant difference in median $\delta^{34}S$ values between interval I and the overlying intervals (p-value = 0.004).

The low $\delta^{34}S$ values observed in intervals II and III along with the similar shifts observed in the bulk carbonate and organic carbon isotopic measurements are consistent with a more open pore-water system, resulting in sulfate being more extensively used as an oxidant within the sediment column during deposition of intervals II and III. This activity would have resulted in the utilization of a higher proportion of the organic matter and is associated with decreased quality of foraminiferal preservation, particularly infilling by ^{12}C-enriched authigenic carbonate. A likely overriding control on these changes (including the change in preservation) is the availability of sulfate in pore fluids. Sulfate is the second most abundant anion in modern seawater (28 m*M*) and is a critical oxidant for the remineralization of organic matter in shallow marine sediments (Kasten and Jørgensen, 2000).

Relative to the modern ocean, Cretaceous seawater is thought to have had lower sulfate concentrations (~10–15 m*M*; Horita et al., 2002; Lowenstein et al., 2003; Berner, 2004). Given that sulfate reducers are obligate anaerobes, anoxic conditions and the availability of suitable organic substrates are required to drive their reductive metabolic activities. The balanced redox reaction may be written as:

$$4CH_2O + SO_4^{2-} + 4H_2O \rightarrow 4HCO_3^- + H_2S + 2H^+.$$

This microbial process releases alkalinity, acidity, and hydrogen sulfide to pore fluids, with the sulfur in the H_2S typically being depleted in ^{34}S (McFadden and Kelly, 2011). The magnitude of fractionation is dependent on factors that control the rate of reduction, including temperature and the availability of sulfate and/or a source of electrons (i.e., organic matter; Brunner and Bernasconi, 2005; Canfield and Farquhar, 2009; Leavitt et al., 2013; Zhelezinskaia et al., 2014). Experiments on modern sulfate reducers (Johnston et al., 2007) show that the magnitude of sulfur isotope fractionation by bacterial sulfate reducers reflects environmental conditions that affect the transport of sulfate into and out of the cells. It has been argued that large fractionations would not be preserved unless pore-water sulfate concentrations were higher than 200 µ*M* (Habicht et al., 2002), and Fe^{2+} was available for the formation of insoluble pyrite (Berner and Raiswell, 1983). This threshold now appears to be an upper limit, as recent observations of modern meromictic lakes (Gomes and Hurtgen, 2013) with SO_4^{2-} as low as 25–100 µ*M* indicate that isotopic fractionation of more than 20‰ is possible.

For the relatively organic-rich lower interval (I) of Site 31, it seems most likely that the up-section increase in $\delta^{34}S$ recorded in pyrite was a function of diffusive sulfate limitation in rapidly accumulating and finely laminated sediments (Zhelezinskaia et al., 2014). Given the relatively high TOC contents (~1%), it is likely that growth rates among sulfate reducers were rapid, and, thus, sulfate was effectively consumed in pore fluids, minimizing the magnitude of sulfur isotope fractionation (Leavitt et al., 2013). The up-section decrease in $\delta^{34}S$ values through the upper two intervals (II and III), however, suggests that sulfate became more widely available in pore fluids. Such a change could have been caused by increased connectivity with the seawater reservoir due to lower sedimentation rates (Huber et al., 2017), or an increase in grain size toward the top of the section (Fig. DR4 [see footnote 1]; Wendler et al., 2016). Additionally, or alternatively, increased connectivity between pore fluids and the overlying seawater reservoir could have reflected an increase in the degree of bioturbation, which is inferred from a shift from generally laminated to more massive fabrics above 28 m (Jiménez Berrocoso et al., 2012; Wendler et al., 2016). However, there does not appear to be any increase in the relative abundance of pyritized burrows above 28 m (Wendler et al., 2016).

Greater sulfate availability would enhance the rate of organic matter remineralization by microbial sulfate reducers. Geochemical models of microbial sulfate reduction (Meister, 2013) indicate that the onset of this metabolic strategy initially lowers pH, which would favor dissolution of carbonate rather than its production; however, as the process continues, pH is stabilized, and saturation increases with the buildup of carbonate alkalinity (Moore et al., 2004), resulting in the precipitation of authigenic carbonate minerals (Schrag et al., 2013).

Foraminiferal Isotopes

Stable isotopic measurements of foraminiferal tests indicate remarkably stable and very warm conditions, assuming an open-ocean environment with an ice-free-appropriate oxygen isotopic value of local surface waters of ~–1‰$_{SMOW}$ (where SMOW is standard mean ocean water; Fig. DR4 [see footnote 1]; MacLeod et al., 2013). High-resolution $\delta^{18}O$ and $\delta^{13}C$ measurements of planktic and benthic foraminifera show little variability throughout the early–middle Turonian and suggest an environment with a moderate thermal gradient between waters at the sea surface and the seafloor (Fig. DR4 [see footnote 1]; MacLeod et al., 2013). A decrease in $\delta^{18}O$ values (~0.5‰) of both planktic and benthic foraminifera starts at ~54 m (in core 32) and suggests warming or freshening of surface and deep water at that time. The shift is correlated with an ~1.5‰ decrease in $\delta^{13}C$ values of planktic and benthic foraminifera, suggesting a parallel decrease in the $\delta^{13}C$ values of the dissolved inorganic carbon pool (Fig. DR4 [see footnote 1]).

Biserial planktic foraminifera consistently exhibit both lower $\delta^{18}O$ values and lower $\delta^{13}C$ values than co-occurring non-biserial planktic species (Fig. DR4 [see footnote 1]; MacLeod et al., 2013). This separation could indicate

vertical and/or seasonal ecological segregation of biserial taxa within the water column. Alternatively, the isotopic differences could indicate spatial segregation, with the biserials living in more coastal environments, but being episodically transported to Site 31 by storm events, eddies created by differential motion across the boundary between an offshore and onshore water mass, or lateral migration of the coastal/offshore water boundary due to sea-level, climatic, or stochastic weather events (Fig. 9). In the discussion, we explore the latter two possibilities, but we note that between ~54 m and 28 m, isotopic ratios among all taxa measured shift toward lower $\delta^{13}C$ and lower $\delta^{18}O$ values. The magnitude of the decrease in $\delta^{18}O$ values of the biserial taxa (~0.5‰) is similar to that of the benthic foraminifera and trochospiral planktic foraminifera, but the shift in $\delta^{13}C$ values of biserial planktic foraminifera (~3‰) is much greater than that of the co-occurring taxa (~1.5‰; MacLeod et al., 2013). This observation supports the likelihood that the biserials were spatially segregated from other planktic taxa.

Shifts in bulk organic and carbonate $\delta^{13}C$ values are consistent with those measured on individual planktic and benthic foraminiferal species (Jiménez Berrocoso et al., 2012). Both bulk $\delta^{13}C_{carb}$ values and $\delta^{13}C_{org}$ values show small variations throughout the lower portion of the section but gradually decrease between ~54 m and ~28 m by 3‰ and 1‰, respectively (Fig. 8). Above 28 m, bulk $\delta^{13}C_{carb}$ values abruptly decrease by almost 3‰, and $\delta^{13}C_{org}$ values decrease by ~2‰. Total organic carbon contents show a similar pattern and gradually decrease from ~1.1% to ~0.8% across the interval of the first shift in $\delta^{13}C$ values, and they drop abruptly to ~0.3% at ~28 m (Fig. 8; Table 1; Jiménez Berrocoso et al., 2012). Together, these observations could reflect a gradual increase up section in the extent of subsurface remineralization of organic matter, especially above 28 m, with the correlated shift in $\delta^{13}C_{org}$ values perhaps reflecting a change in the sources of organic matter. Invoking increased remineralization up section corresponds well with the model proposed earlier to explain stratigraphic patterns in $\delta^{34}S$ values.

Biomarkers

Similar to the palynomorph assemblage and consistent with previous findings involving Eocene sediments from Tanzania (Pearson et al., 2004; van Dongen et al., 2006), biomarkers are well preserved and suggest dominantly terrestrial sources for preserved organic matter. Long-chained *n*-alkanes (i.e., $\geq C_{25}$-*n*-alkanes) with an odd-to-even predominance (OEP) are the most abundant biomarkers found (Figs. 10 and 11; Table DR5 [see footnote 1]). Other common constituents include the C_{29}–C_{32} 17β(H),21β(H)-hopanes, C_{29} olean-12-ene, C_{30} olean-12-ene (or taraxerene), and the C_{27}–C_{29} 10α-diaster-13(17)-enes (S and R epimers present in all samples; Fig. 11). Minor constituents observed throughout Site 31 include the C_{29}–C_{31} hop-17(21)-enes, the C_{29}–C_{31} 17α(H),21β(H)-hopanes, C_{27} 22,29,30-trinor-18α-neohopane (Ts), C_{27} 22,29,30-trinor-17α-hopane (Tm), and the 4α-methylsterols.

The abundant long-chained *n*-alkanes that exhibit an OEP likely derive from higher-plant leaf waxes (Figs. 10 and 11; Eglinton and Hamilton, 1967). In addition, the presence of triterpenes (identified here as either taraxerene or olean-12-ene) indicates that angiosperms contributed to the terrestrially derived organic material (Crane and Lidgard, 1989; Rullkötter et al., 1994). Further, C_{29}-diaster-13(17)-enes are more common than the C_{27} and C_{28}

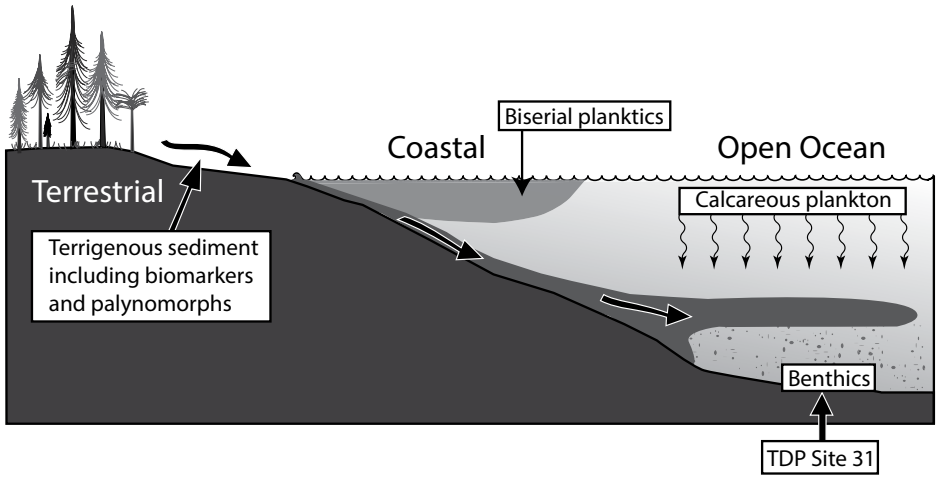

Figure 9. Cartoon cross section illustrating the proposed depositional regime during the Turonian at Tanzania Drilling Project (TDP) Site 31.

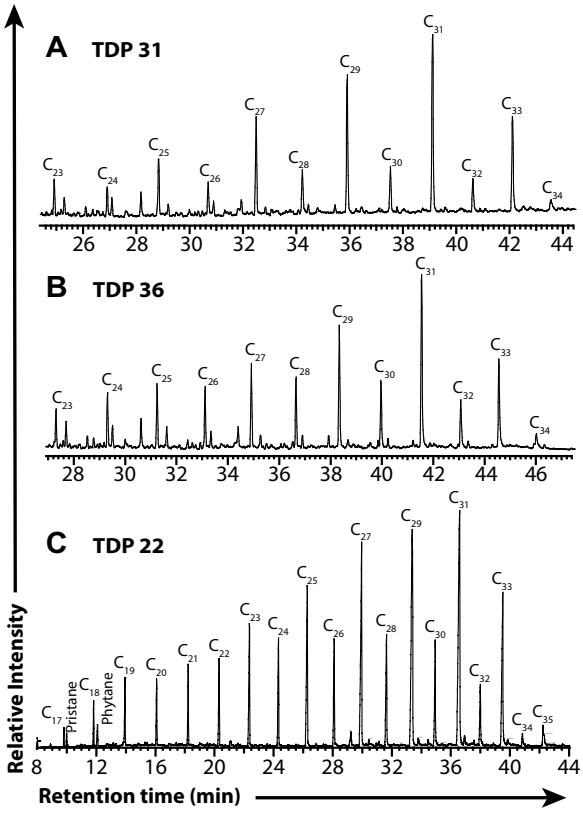

Figure 10. Mass chromatogram (*m/z* 57) showing *n*-alkanes and illustrating an odd-to-even carbon number predominance (OEP) among *n*-alkanes at Tanzania Drilling Project (TDP) Sites 31 (A), 36 (B), and 22 (C).

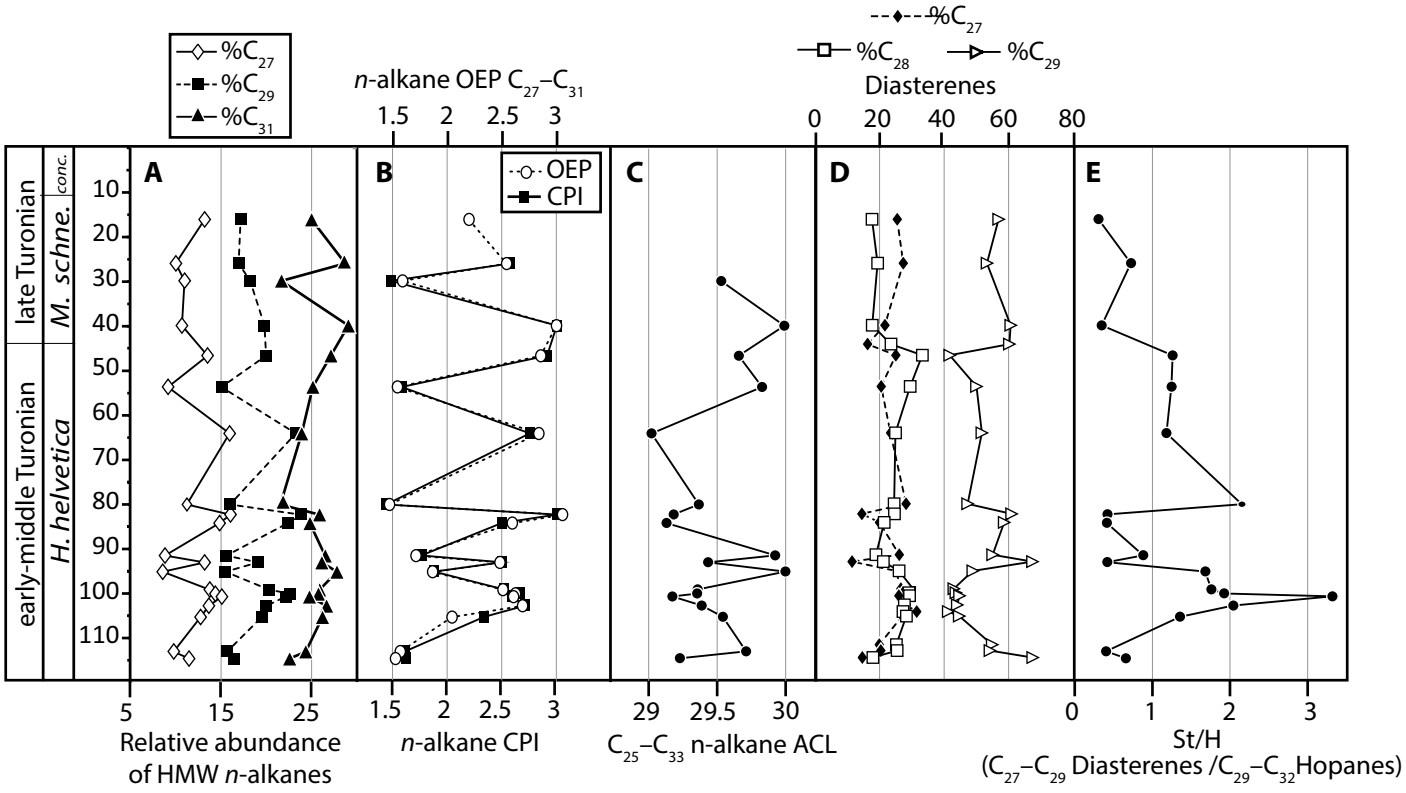

Figure 11. Depth profiles of relevant biomarker ratios from Tanzania Drilling Project (TDP) Site 31. (A) Relative abundance of high-molecular-weight (HMW) *n*-alkanes relative to C_{26}–C_{33} *n*-alkanes, (B) odd-to-even predominance (OEP) and carbon preference index (CPI), (C) C_{25}–C_{33} *n*-alkane average chain length (ACL), (D) percent relative abundance of C_{27}–C_{29} diasterenes, (E) the ratio of 10α-diaster-13(17)-enes to C_{29}–C_{32} 17β(H),21β(H)-hopanes (St/H). All equations used to calculate the reported ratios are included in Table 2. Abbreviations are as follows: *H. helvetica*—*Helvetoglobotruncana helvetica*, *M. schne.*—*Marginotruncana schneegansi*, and *conc.*—*Dicarinella concavata*.

diaster-13(17)-enes (Figs. 10 and 12), a pattern thought to be typical of environments with abundant higher-plant input (Huang and Meinschein, 1979). Although C_{29} sterols can also be produced by marine organisms (Volkman et al., 1981, 2015; Volkman, 1986), their high relative proportion here is likely reflective of terrestrial higher-plant input, consistent with the other observations for abundant terrestrially derived material (Fig. 12).

In contrast, biomarkers indicative of marine organic matter are relatively rare. Diaster-13(17)-enes derive from sterols that are produced by both terrestrial and marine eukaryotes, but the presence of C_{27} and C_{28} diasterenes suggests some of the organic matter was likely of marine origin (Volkman, 1986; Killops and Killops, 2005). Further, 4α-methylsterols are present, albeit in low concentrations, and are likely derived from marine dinoflagellates and/or diatoms (de Leeuw et al., 1983; Robinson et al., 1984; Volkman et al., 1990). The presence of steroids distinguishes these sediments from previously studied Eocene sediments from Tanzania (van Dongen et al., 2006).

There are no obvious trends among biomarkers through or within Site 31, but sampling resolution is relatively low, making it difficult to rule out high-frequency environmental or sedimentological variations that might mask general trends. Carbon preference index, OEP, and average chain length are all variable throughout the section but show no consistent trends (Fig. 11; Table 2). Similarly, relative proportions of C_{27}–C_{29} diaster-13(17)-enes, which would indi-

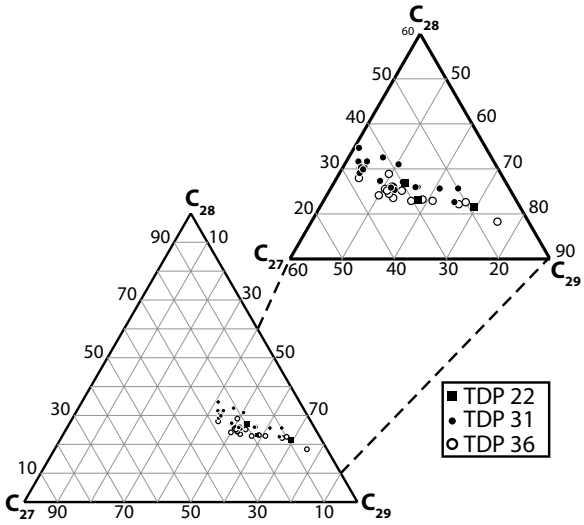

Figure 12. Ternary plot with relative proportions of C_{27}, C_{28}, and C_{29}-diasterenes for Tanzania Drilling Project (TDP) Sites 22, 31, and 36.

TABLE 2. RELEVANT BIOMARKER EQUATIONS, WHERE PEAK AREAS WERE ALL MEASURED USING TOTAL ION CHROMATOGRAMS

Relative abundance of high-molecular-weight (>C_{25}) *n*-alkanes	$\left(\frac{nC_{26+i}}{nC_{26}+nC_{27}+\ldots nC_{32}+nC_{33}}\right)\times 100 \quad i = 0,\ 2,\ 4$
Odd-over-even predominance (OEP) (Scalan and Smith, 1970)	$\frac{C_{27}+6C_{29}+C_{31}}{4C_{28}+4C_{30}}$
Carbon preference index (CPI) (Bray and Evans, 1961; Handley et al., 2012)	$\frac{2\times(nC_{25}+nC_{27}+nC_{29}+nC_{31})}{\left[nC_{24}+2\times(nC_{26}+nC_{28}+nC_{30})+nC_{32}\right]}$
Average chain length (ACL) (Jeng, 2006)	$\frac{25(nC_{25})+27(nC_{27})+29(nC_{29})+31(nC_{31})+33(nC_{33})}{nC_{25}+nC_{27}+nC_{29}+nC_{31}+nC_{33}}$
Relative abundance of C_{27}–$C_{29}\Delta^{13(17)}$, (20S), 10α-diasterenes	$\left(\frac{C_i}{C_{27}+C_{28}+C_{29}}\right)\times 100 \quad i = 27,\ 28,\ 29$
Diasterene/hopane ratio (St/H)	$\frac{\Sigma C_{27}-C_{29}\Delta^4,\ (20S),\ 10\alpha\text{-diasterenes}}{\Sigma C_{29}-C_{32}\ 17\beta,\ 21\beta\text{-hopanes}}$

cate a shift in organic matter sources through the section, show no obvious trends, but subtle patterns do exist among diaster-13(17)ene/ββ-hopane ratios, which are commonly used to infer shifts between marine and terrestrial sources of organic matter (with higher values associated with a greater proportion of more marine organic matter and vice versa; Fig. 11; Table 2; e.g., Peters and Moldowan, 1993; Peters et al., 2005). Diaster-13(17)-ene/ββ-hopane ratios are relatively high below 40 m, whereas ratios are low at the top and bottom of the section as well as between 82 and 93 m. Similar subtle shifts occur in the proportions of diaster-13(17)-enes at the same depths, and collectively these variations could indicate a progressive decrease in the proportion of marine relative to terrestrial organic matter (Fig. 11).

Consistent with excellent preservation among microfossils, the biomarkers are quite immature. The most abundant hopanes present throughout Site 31 are C_{29}–C_{32} ββ-hopanes. The primary 17β(H),21β(H) isomerization indicates very low thermal maturity (Peters and Moldowan, 1993; Killops and Killops, 2005). The predominance of diasterenes is also useful in constraining the diagenetic history of the site, as the transformation from sterenes to diasterenes generally occurs when there is extensive clay-catalyzed rearrangement during early diagenesis (Marynowski et al., 2007).

Sedimentological Observations

Sedimentary fabrics lack any indicators of wave activity, and there is a general lack of evidence for traction and/or gravity transport, observations consistent with an offshore, low-energy depositional environment (Jiménez Berrocoso et al., 2010, 2012, 2015). The most common sedimentary structures present are thinly bedded to laminated intervals and occasional evidence of soft-sediment deformation (Fig. 3). The scarcity of sedimentary structures indicating event deposits, coupled with preservation of laminae and subtle bedding contacts, indicates a general lack of deep bioturbation throughout most of the section and relatively high sedimentation rates. To have such conditions at outer-shelf depths suggests that the sediments were not delivered directly to the seafloor via a fluvial system but rather settled from a turbid water column (Jiménez Berrocoso et al., 2012, 2015). Because planktic foraminiferal assemblages indicate nutrient-poor surface waters, and such waters tend to be clear, we suggest that a majority of the terrigenous material was transported in subsurface flows (Fig. 9). A similar combination of traits associated with open-ocean and nearshore conditions was invoked to explain excellent preservation of nannofossils in Eocene–Oligocene sediments (Dunkley Jones et al., 2009). Given the available data, it is difficult to determine how much, if any, terrestrial material may have been delivered to the system via eolian inputs.

Grain size is generally fine and ranges from clay- to silt-sized particles, with minor fine quartz sand as well as sand-size foraminiferal tests (Fig. DR4 [see footnote 1]; Jiménez Berrocoso et al., 2012; Wendler et al., 2016). The scarcity of marine organic carbon, despite common marine microfossils and excellent organic matter preservation, suggests marine organic matter was efficiently recycled in the water column and/or at the seafloor. If this was the case, then less labile, terrestrial organic matter would have been the only organic carbon that would have survived below the sediment-water interface. Minimal burrowing combined with fine grain size would reduce permeability and have limited oxygen and sulfate recharge of pore waters. These conditions, in turn, would limit bacterial degradation of the refractory terrestrial organic matter. Quantitative grain-size data from Wendler et al. (2016) are presented in Supplementary Figure DR4 as percentage grain-size fraction (i.e., clay = 0.4–4 μm, silt = 4–63 μm, sand = 63–2000 μm). Grain size coarsens between 42 m and 28 m (Fig. DR4 [see footnote 1]; Wendler et al., 2016). In these measurements, the relative proportion of sand-sized particles increases ~9× across the interval (from 3% to 27%), clay decreases by about half (from 31% to 15%), and silt decreases slightly (from 66% to 58%). This change is dramatic, but it is difficult to distinguish between the relative contributions of terrigenous grains, sand-sized foraminifera, and sedimentary aggregates to the measured increase in the proportion of sand-sized grains. Along these lines, semiquantitative observations indicate medium- to coarse-sand–sized quartz is common to abundant throughout the section (Wendler et al., 2016), and no increase in grain size was recognized in the initial core descriptions (Jiménez Berrocoso et al., 2012). The increase in measured grain size, though, does correlate closely with a pronounced decline in foraminiferal preservation, as well as with faunal and isotopic shifts in planktic and benthic foraminifera, a shift toward lower $\delta^{34}S$ values, and an initial decrease in bulk $\delta^{13}C_{carb}$ values. Possible interpretations include: a shift in sediment supply, a shift in sediment routing through changes like channel avulsion, shifts in local bathymetry, climatically forced changes in local oceanographic conditions, and/or paleoecological changes that resulted in an increase in the input of sand-sized foraminifera.

DISCUSSION OF DEPOSITIONAL SETTING

Deposition at Site 31 was dominated by largely decoupled terrestrial and marine inputs. Fine grain sizes and shallow burial—traditionally invoked explanations for excellent microfossil preservation—are present throughout, but preservation is not consistently excellent. We argue that changes in sediment column conditions were critically important for promoting excellent preservation in some intervals but not others. By suggesting decoupled terrestrial and marine inputs, we mean many observations indicate either a dominantly terrestrial signature or a dominantly marine signature with little evidence of mixing between the two. Further, inputs from marginal marine or shallow-water environments appear to have been minor. Evidence for a strong influence of terrestrial sources that were minimally affected by marine processes includes excellently preserved organic matter showing common terrestrial biomarkers but few marine indicators, palynomorph assemblages dominated by spores and pollen, and high sedimentation rates (several cm/1000 yr;

MacLeod et al., 2013). In contrast, calcareous microfossils suggest a relatively deep, open-ocean environment with oligotrophic surface-water conditions overlying a seafloor with a diverse assemblage of outer-shelf to upper-slope benthic foraminifera (Wendler et al., 2016; Huber et al., 2017). Reworked shallow-water or estuarine taxa are absent. A general lack of sedimentary structures indicating current reworking or large-scale downslope transport is consistent with a hemipelagic style of deposition without modification by coastal, shallow-water or deep-basin processes (Jiménez Berrocoso et al., 2010, 2012, 2015).

During the deposition of the lower 86 m of the Turonian sediments recovered from TDP Site 31, there seems to have been low levels of infaunal biological activity. Although benthic foraminifera are common and include both epifaunal and infaunal taxa (Wendler et al., 2013, 2016), indicating ample food supply and a normally oxygenated seafloor, bioturbation intensity was low and, in most intervals, absent at the macroscopic scale. Throughout the section, discrete burrows are rare to absent, and subtle bedding contacts and laminations are often preserved (Fig. 3; Jiménez Berrocoso et al., 2012). Similarly, preservation of coccospheres in Paleogene-aged sections from Tanzania has been associated with very low levels of bioturbation (Bown et al., 2014). Fine grain sizes could have limited permeability in the sediment column, and, especially in the absence of extensive burrowing, high sedimentation rates would have resulted in both a relatively short residence time of sediments in the biologically active layer and little exchange between pore and bottom waters. Consistent with this interpretation, sulfur isotopes of pyrite are variable and are often high in the interval with excellent preservation (Figs. 8 and 9). These high $\delta^{34}S$ values suggest pore waters were effectively isolated from the seawater sulfate reservoir. Rapid burial and low biological activity within the subsurface (limited by oxygen and sulfate availability) would mean calcareous and organic microfossils were buried quickly in low-permeability sediments where pore waters had not evolved far from seawater conditions in variables like pH, alkalinity, and temperature that might have driven alteration of calcareous microfossils and terrigenous organic matter.

In the surface waters above Site 31, a diverse open-ocean planktic community thrived and created a sufficiently high flux of shells to the seafloor for foraminifera and nannofossils to be present in moderate abundances in most samples despite high sedimentation rates. The presence of a typical open-ocean benthic foraminiferal community (Wendler et al., 2016) suggests a high flux of sinking marine organic matter consistent with the abundance and diversity of planktic microfossils. However, based on the scarcity of marine biomarkers and the lack of traces that would indicate a thriving community of both marine and sediment-mining detritivores, we suggest this marine-sourced organic matter was almost completely recycled in the water column and/or near the seafloor, a scenario that fits well with evidence for enhanced rates of organic matter remineralization during periods with high temperatures such as that proposed for the Eocene (John et al., 2013). Degradation of the marine organic matter that reached the seafloor may have depleted pore waters of O_2 and SO_4^{2-} through aerobic and anaerobic microbial activities close to the sediment-water interface. Terrestrial organic matter preferentially survived remineralization, likely due to its composition and/or because much of it was adsorbed onto fine terrigenous grains, making it less available (Blair and Aller, 2012). If levels of biological activity in the subsurface were low, and there was little circulation of pore waters, pore-water chemistry would not change greatly with depth; thus, carbonate dissolution, recrystallization, and reprecipitation would be minor. Generally high bulk $\delta^{13}C_{carb}$ values in the interval of best preservation (i.e., interval I; Fig. 8) are consistent with minimal formation of diagenetic ^{13}C-depleted carbonate. The final contributor that led to the high quality of preservation of the minimally altered terrestrial organic matter and calcareous microfossils was a lack of deep burial and lack of exposure to high temperatures and pressures, as attested by the low thermal maturity of organic matter.

Consistent with our model invoking a bimodal (terrestrial and offshore marine) sediment budget, the isotopic values in biserial planktic foraminifera and the relatively high proportion of small morphotypes of several trochospiral planktic species suggest that Site 31 was close to marginal marine environments, despite the dominantly open-ocean character of the calcareous microfossil assemblages. Low $\delta^{18}O$ values among biserial taxa might be interpreted as indicating preference of these taxa for the warmest (shallowest) surface waters and/or population peaks during the warmest seasons (MacLeod et al., 2013; Wendler et al., 2013). However, relatively low $\delta^{13}C$ values among biserial taxa are difficult to fit into a simple depth-stratification model because warm-season surface-water dissolved inorganic carbon (DIC) should have high $\delta^{13}C$ values (e.g., Spero, 1992; Haynes et al., 2015).

Disequilibrium fractionation has been proposed to explain anomalous $\delta^{13}C$ values in biserial taxa (e.g., Abramovich et al., 2003; Wendler et al., 2013, 2016). Disequilibrium in Tanzanian specimens would presumably need to result from low-$\delta^{13}C$ metabolic CO_2 being used during test formation because kinetic fractionation during hypothetical rapid growth (also proposed to explain biserial foraminiferal isotopic values) should produce positively correlated $\delta^{13}C$ and $\delta^{18}O$ values (e.g., McConnaughey, 1989a, 1989b), which we do not observe (Fig. 13). An alternative model, which we prefer, is that the biserial taxa precipitated their tests in approximate equilibrium with local seawater but were not living in the same waters as the other planktic foraminifera. If the biserial taxa analyzed had a preference for living in coastal waters (Leckie, 1987) but episodically reached the seafloor at Site 31 due to seasonal or interannual migration of water mass boundaries or due to transport during or after extreme weather events, their shell chemistry might reflect a contribution of both low $\delta^{13}C_{DIC}$ and low $\delta^{18}O$ of freshwater runoff, and they would plot in a separate field from planktic foraminifera living in oligotrophic, offshore water masses.

For terrigenous material, including terrestrial palynomorphs and higher-plant biomarkers, we suggest transport either via discrete, hyperpycnal plumes moving under clear, nutrient-poor surface waters, or as a more general and deeper turbid wedge in which the upper boundary sloped downward in the oceanward direction under clear, nutrient-poor surface waters (Fig. 9). The limited number of massive sandstone beds present in Site 31 and in other Turonian sediments cored in Tanzania could have been deposited when turbid waters transported a higher fraction of sand-sized grains offshore.

Hot dry conditions inferred from pollen and spores could have enhanced offshore flows. High evaporation during dry seasons might have produced shelfal waters that were saline enough to carry a suspended load delivered by fluvial processes offshore as density cascades (Wilson and Roberts, 1995). Alternatively, turbid fluvial waters mixed with coastal waters and/or fluvial sediments resuspended by storm waves may have been prevalent and moved significant sediment offshore as midwater plumes, which could have also evolved into a turbid wedge basinward. The route any midwater and/or deeper turbid wedge traveled would have been influenced by shoreline-parallel currents. Regardless of uncertainty concerning specific transport geometry, the general lack of structures indicative of traction currents and/or gravity flows seems to rule out bottom current and bed-load transport as important processes for moving sediments to Site 31 (Fig. 9).

Differences between Site 31 and nearby Sites 22 and 36, which also contain exceptionally well-preserved Turonian calcareous microfos-

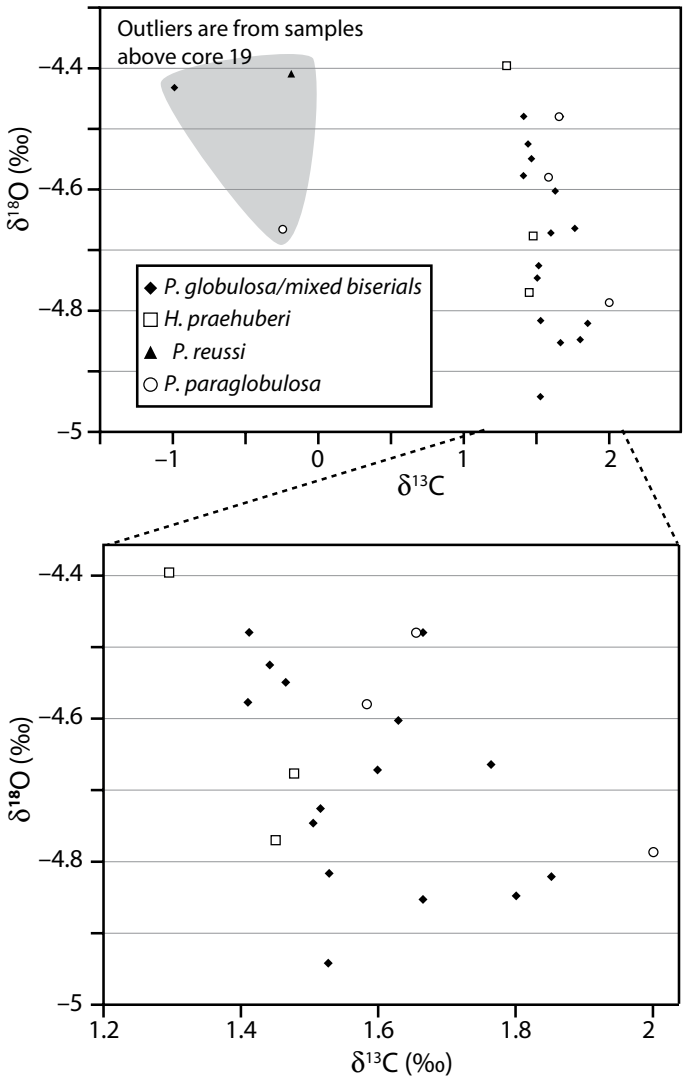

Figure 13. Cross-plot of $\delta^{13}C$ (‰) and $\delta^{18}O$ (‰) values of biserial planktic foraminifera from Tanzania Drilling Project (TDP) Site 31. The top panel includes all available data for biserials from Site 31, and the lower panel is a close-up illustration that excludes specimens that are suspected to be diagenetically altered above core 19. Abbreviations are as follows: *P.—Planoheterohelix*, *H.—Huberella*. Isotope data is used with permission from MacLeod et al. (2013).

sils, are consistent with the bimodal depositional model. The three sites are within 5.2 km of each other, and all three preserve clay-rich terrigenous sediments containing diverse, open-ocean planktic foraminiferal assemblages suggestive of nutrient-poor surface waters. Although biomarker analysis for Sites 22 and 36 was done at lower resolution than Site 31, both sites show an obvious abundance of long chained *n*-alkanes with OEP, and an abundance of C_{29} diasterenes relative to the C_{27} and C_{28} diasterenes, suggesting an abundance of terrestrially derived organic material (Figs. 10 and 12). The average grain sizes at both Sites 22 (21% clay, 70% silt, 9% sand) and 36 (18% clay, 78% silt, 3% sand) are coarser than in the lower 86 m at Site 31 (33% clay, 65% silt, 1% sand) but finer than in the upper, less-well-preserved portions of Site 31 (15% clay, 58% silt, 27% sand; Fig. DR4 [see footnote 1]; Wendler et al., 2016). Further, at Site 22, $\delta^{18}O$ values of benthic foraminifera are consistently ~1‰ lower than at Site 31 (MacLeod et al., 2013), and the ratio of terrestrial- to marine-derived palynomorphs is slightly higher at Site 36 than at Site 31 (Figs. 7 and 14). Foraminiferal isotopes have not been measured for Site 36 samples, and palynomorphs have not been characterized for Site 22 samples.

The differences among sites suggest that Sites 22 and 36 were generally closer to terrigenous sources than Site 31. However, considering inferred pelagic/hemipelagic, outer-shelf to upper-slope depositional regimes for all sites, the distances between sites are too small for variations to be reasonably explained purely by distance from the coastline. This paradox is resolved by the turbid wedge/or hyperpycnal flow models, because depth and/or perpendicular distance to the coast are not the most important variables. That is, if subsurface flows had lateral variability not simply related to the orthogonal distance to the coast, differences in the distance from the axis of flow could result in measurable differences in grain size and sediment character among otherwise very similar sites. If so, changes through a section might reflect local changes in sediment routing (e.g., channel avulsion in nearby river systems, offshore bathymetric changes, or geostrophic currents). Alternatively, regional changes in hydrology (e.g., increased runoff during humid phases or shifts in ocean currents), or global events (e.g., eustatic sea-level changes or climatic shifts affecting circulation with local effects) could also be invoked to explain stratigraphic changes in the sediments at Site 31.

The decline in the quality of preservation in the upper part of the section at Site 31 that persists into the early Campanian at other sites in the region, coupled with increased grain size (Wendler et al., 2016), higher abundances of biserial planktic foraminifera (Haynes et al., 2015), calcareous nannofossil species turnover (Huber et al., 2017), and decreases in $\delta^{13}C$ and $\delta^{18}O$ values (Jiménez Berrocoso et al., 2012; MacLeod et al., 2013) could reflect a variety of changes that increased subsurface biological activity and changes in diagenetic conditions. The abruptness of these shifts may be an artifact of a short hiatus suggested by nannofossil distributions, but the ultimate cause for the change in sediment character—the shift to a depositional environment where there was improved connectivity between pore waters and seawater—seems to be the best explanation for the temporary (latest Turonian–early Campanian) closure of the lagerstätte taphonomic window in samples from the Lindi region, even though dominant lithologies remained fine (clayey siltstones), and burial history was unchanged.

CONCLUSIONS

Low biological activity in the sediment column seems to be the most important proximate factor controlling where excellent preservation occurred throughout much of the Turonian sedimentary sequence in Tanzania. Low biological

activity is indicated by scarcity of bioturbation and generally high $\delta^{34}S$ values in pyrite in the interval with the best preservation, suggesting rapid depletion of pore-water sulfate after burial, thus limiting bacterial sulfate reduction and associated organic matter remineralization. This limitation, in turn, led to burial of microfossils in contact with pore waters that had not evolved greatly away from conditions in contemporary bottom waters with regard to several variables important for carbonate stability (e.g., pH, alkalinity, temperature). Factors that likely promoted these burial conditions include high depositional rates of fine-grained sediments (leading to rapid burial and low permeability, isolating pore waters from seawater, and preventing oxidation of palynomorphs) and near-complete recycling of marine organic matter (as indicated by a scarcity of marine biomarkers), leaving only relatively unreactive terrestrial organic matter in the sediment column. Close proximity between terrestrial inputs and the open-ocean environment along the Tanzanian paleomargin was likely needed to permit a high flux of terrigenous material to the seafloor below mostly oligotrophic surface waters that were productive enough to be the source of a reasonably abundant, diverse calcareous microfossil assemblage. Finally, shallow burial depth was an important contributing factor, as burial temperatures were never high enough to greatly alter the remaining organic matter or lead to significant abiotic recrystallization of carbonates.

We propose that the shift to more poorly preserved calcareous microfossils in the mid–late Turonian resulted from an increase in biological activity within the sediment column, particularly increased microbial sulfate reduction leading to higher remineralization of sedimentary organic matter, as well as carbonate dissolution and reprecipitation. In the upper portion of the section in which quality of preservation declines, $\delta^{34}S$ decreases (suggesting relatively open-system behavior of pore-water sulfate), organic carbon content decreases, and the $\delta^{13}C$ of bulk carbonate decreases (consistent with remineralized organic carbon being incorporated into secondary carbonate).

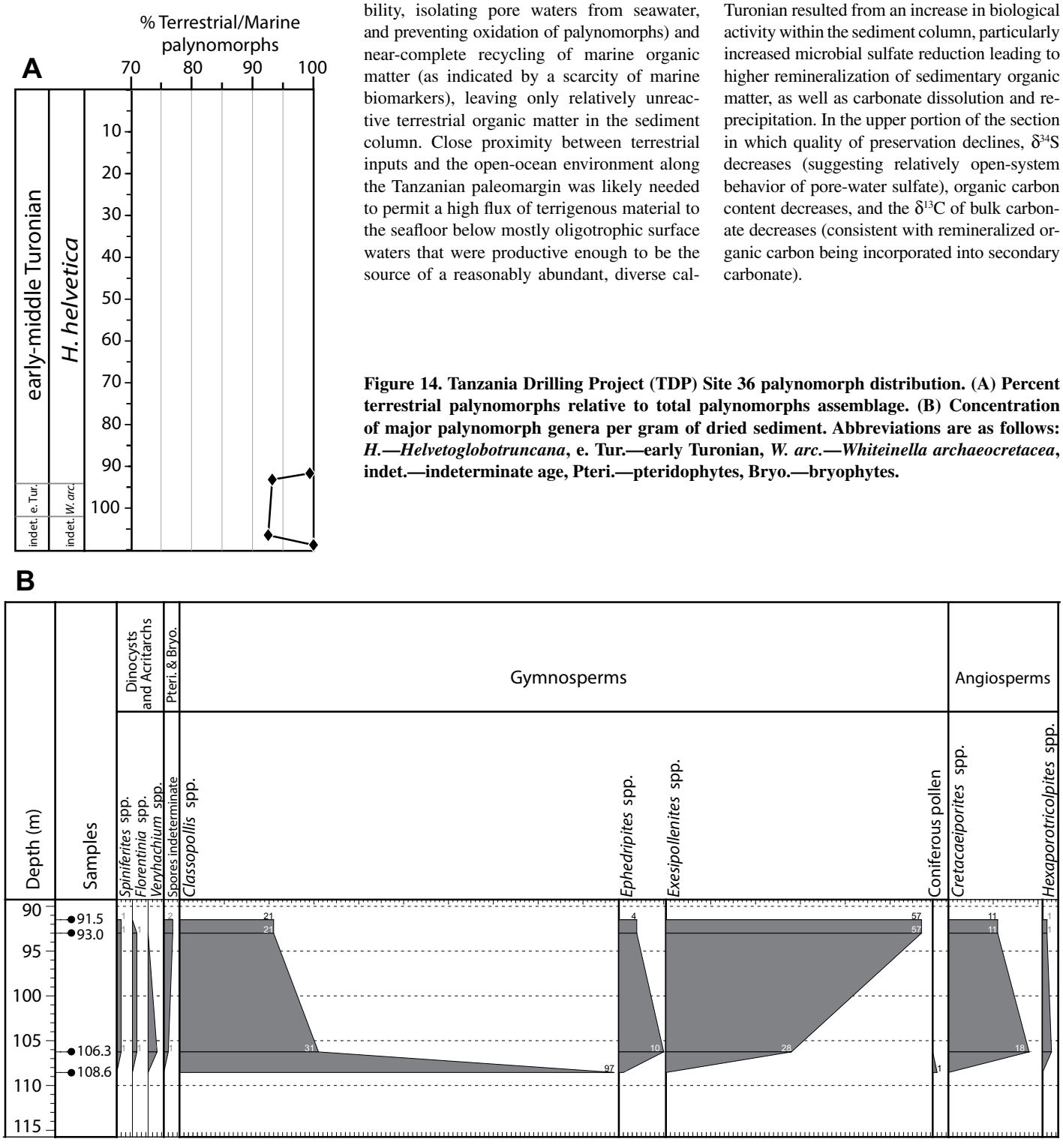

Figure 14. Tanzania Drilling Project (TDP) Site 36 palynomorph distribution. (A) Percent terrestrial palynomorphs relative to total palynomorphs assemblage. (B) Concentration of major palynomorph genera per gram of dried sediment. Abbreviations are as follows: *H.—Helvetoglobotruncana*, e. Tur.—early Turonian, *W. arc.—Whiteinella archaeocretacea*, indet.—indeterminate age, Pteri.—pteridophytes, Bryo.—bryophytes.

ACKNOWLEDGMENTS

We greatly appreciate Loren Petruny and fellow interns at the Smithsonian Institution National Museum of Natural History for help with picking foraminifera at Tanzania Drilling Project (TDP) Sites 22, 31, and 36. Ines Wendler at the University of Bremen, Germany, provided helpful comments and contributed to picking and counting benthic foraminifera at Site 31. Laboratory Managers Rebecca Plummer and Yongbo Peng at the University of Maryland helped to carry out sulfur abundance and isotopic analyses. We also thank James Farquhar at the University of Maryland for the use of his laboratory to do CRS extractions.

REFERENCES CITED

Abramovich, S., Keller, G., Stüben, D., and Berner, Z., 2003, Characterization of late Campanian and Maastrichtian planktonic foraminifera depth habitats and vital activities based on stable isotopes: Palaeogeography, Palaeoclimatology, Palaeoecology, v. 202, p. 1–29, doi:10.1016/S0031-0182(03)00572-8.

Akyuz, I., Warny, S., Oyebode, F., and Bhattacharya, J., 2015, Palynology of the Turonian Ferron-Notom Sandstone, Utah: Identification of marine flooding surfaces and Milankovitch cycles in subtropical, ever-wet, paralic to non-marine paleoenvironments: Palynology, v. 40, p. 122–136, doi:10.1080/01916122.2015.1014525.

Berner, R.A., 2004, The Phanerozoic Carbon Cycle: CO_2 and O_2: Oxford, UK, Oxford University Press, 158 p.

Berner, R.A., and Raiswell, R., 1983, Burial of organic carbon and pyrite sulfur in sediments over Phanerozoic time: A new theory: Geochimica et Cosmochimica Acta, v. 47, p. 855–862, doi:10.1016/0016-7037(83)90151-5.

Blair, N.E., and Aller, R.C., 2012, Organic carbon in the marine environment: Annual Review of Marine Science, v. 4, p. 401–423, doi:10.1146/annurev-marine-120709-142717.

Bolli, H.M., 1945, Zur Stratigraphie der oberen Kreide in den höheren helvetischen Decken: Eclogae Geologicae Helvetiae, v. 37, p. 217–328.

Bown, P.R., Dunkley Jones, T., Lees, J.A., Randell, R.D., Mizzi, J.A., Pearson, P.N., Coxall, H.K., Young, J.R., Nicholas, C.J., Karega, A., Singano, J., and Wade, B.S., 2008, A Paleogene calcareous microfossil Konservat–Lagerstätte from the Kilwa Group of coastal Tanzania: Geological Society of America Bulletin, v. 120, no. 1–2, p. 3–12, doi:10.1130/B26261.1.

Bown, P.R., Gibbs, S.J., Sheward, R., O'Dea, S., and Higgins, D., 2014, Searching for cells: The potential of fossil coccospheres in coccolithophore research: Journal of Nannoplankton Research, v. 34, special issue, p. 5–22.

Bray, E.E., Evans, E.D., 1961, Distribution of *n*-paraffins as a clue to recognition of source beds: Geochimica et Cosmochimica Acta, v. 22, p. 2–15.

Brown, C., 2008, Palynological techniques, *in* Riding, J., and Warny, S., eds.: Dallas, American Association of Stratigraphic Palynologists Foundation Special Publication, 137 p.

Brunner, B., and Bernasconi, S.M., 2005, A revised isotope fractionation model for dissimilatory sulfate reduction in sulfate reducing bacteria: Geochimica et Cosmochimica Acta, v. 69, p. 4759–4771, doi:10.1016/j.gca.2005.04.015.

Burnett, J.A. (with contributions from Gallagher, L.T., and Hampton, M.J.), 1998, Upper Cretaceous, *in* Bown, P.R., ed., Calcareous Nannofossil Biostratigraphy: London, British Micropalaeontological Society Publications Series, Chapman and Hall/Kluwer Academic Publishers, p. 132–199.

Canfield, D.E., and Farquhar, J., 2009, Animal evolution, bioturbation, and the sulfate concentration of the oceans: Proceedings of the National Academy of Sciences of the United States of America, v. 106, p. 8123–8127, doi:10.1073/pnas.0902037106.

Canfield, D.E., Raiswell, R., Westrich, J.T., Reaves, C.M., and Berner, R.A., 1986, The use of chromium reduction in the analysis of reduced inorganic sulfur in sediments and shales: Chemical Geology, v. 54, p. 149–155, doi:10.1016/0009-2541(86)90078-1.

Corbett, M.J., Watkins, D.K., and Pospichal, J.J., 2014, Quantitative analysis of calcareous nannofossil bioevents of the Late Cretaceous (late Cenomanian–Coniacian) Western Interior Seaway and their reliability in established zonation schemes: Marine Micropaleontology, v. 109, p. 30–45, doi:10.1016/j.marmicro.2014.04.002.

Crane, P.R., and Lidgard, S., 1989, Angiosperm diversification and paleolatitudinal gradients in Cretaceous floristic diversity: Science, v. 246, no. 4930, p. 675–678, doi:10.1126/science.246.4930.675.

Cushman, J.A., 1938, Cretaceous species of *Gümbelina* and related genera: Contributions from the Cushman Laboratory for Foraminiferal Research, v. 14, p. 2–28.

de Leeuw, J.W., Rijpstra, W.I.C., Schenck, P.A., and Volkman, J.K., 1983, Free, esterfied and residual bound sterols in Black Sea Unit I sediments: Geochimica et Cosmochimica Acta, v. 47, p. 455–465, doi:10.1016/0016-7037(83)90268-5.

Dunkley Jones, T., Bown, P.R., and Pearson, P.N., 2009, Exceptionally well preserved Upper Eocene to Lower Oligocene calcareous nannofossils (Prymnesiophycidae) from the Pande Formation (Kilwa Group) Tanzania: Journal of Systematic Palaeontology, v. 7, p. 359–411, doi:10.1017/S1477201909990010.

Eglinton, G., and Hamilton, R.J., 1967, Leaf epicuticular waxes: Science, v. 156, no. 3780, p. 1322–1335, doi:10.1126/science.156.3780.1322.

Falzoni, F., Petrizzo, M.R., MacLeod, K.G., and Huber, B.T., 2013, Santonian–Campanian planktonic foraminifera from Tanzania, Shatsky Rise and Exmouth Plateau: Species depth ecology and paleoceanographic inferences: Marine Micropaleontology, v. 103, p. 15–29, doi:10.1016/j.marmicro.2013.07.003.

Gandolfi, R., 1942, Ricerche micropaleontologiche e stratigraphfiche sulla Scaglia e sul flysch Cretacici dei Dintorni di Balerna (Canton Ticino): Rivista Italiana Paleontologia, v. 48, p. 1–160.

Garzon, S., Warny, S., and Bart, P.J., 2012, A palynological and sequence-stratigraphic study of Santonian–Maastrichtian strata from the Upper Magdalena Valley basin in central Colombia: Palynology, v. 36, no. 1, p. 112–133, doi:10.1080/01916122.2012.675147.

Gibson, T.G., 1989, Planktonic benthonic foraminiferal ratios: Modern patterns and Tertiary applicability: Marine Micropaleontology, v. 15, p. 29–52, doi:10.1016/0377-8398(89)90003-0.

Gomes, M.L., and Hurtgen, M.T., 2013, Sulfur isotope systematics of a euxinic, low-sulfate lake: Evaluating the importance of the reservoir effect in modern and ancient oceans: Geology, v. 41, p. 663–666, doi:10.1130/G34187.1.

Habicht, K.S., Gade, M., Thamdrup, B., Berg, P., and Canfield, D.E., 2002, Calibration of sulfate levels in the Archaean Ocean: Science, v. 298, p. 2372–2374, doi:10.1126/science.1078265.

Handley, L., O'Halloran, A., Pearson, P.N., Hawkins, E., Nicholas, C.J., Schouten, S., McMillian, I.K., and Pancost, R.D., 2012, Changes in the hydrological cycle in tropical East Africa during the Paleocene-Eocene thermal maximum: Palaeogeography, Palaeoclimatology, Palaeoecology, v. 329–330, p. 10–21, doi:10.1016/j.palaeo.2012.02.002.

Haynes, S.J., Huber, B.T., and MacLeod, K.G., 2015, Evolution and phylogeny of Mid-Cretaceous (Albian–Coniacian) biserial planktonic foraminifera: Journal of Foraminiferal Research, v. 45, no. 1, p. 42–81, doi:10.2113/gsjfr.45.1.42.

Horita, J., Zimmermann, H., and Holland, H.D., 2002, Chemical evolution of seawater during the Phanerozoic: Implications from the record of marine evaporites: Geochimica et Cosmochimica Acta, v. 66, p. 3733–3756, doi:10.1016/S0016-7037(01)00884-5.

Huang, W.Y., and Meinschein, W.G., 1979, Sterols as ecological indicators: Geochimica et Cosmochimica Acta, v. 43, p. 739–745, doi:10.1016/0016-7037(79)90257-6.

Huber, B.T., and Petrizzo, M.R., 2014, Evolution and taxonomic study of the Cretaceous planktonic foraminifer Genus *Helvetoglobotruncana* Reiss, 1957: Journal of Foraminiferal Research, v. 44, no. 1, p. 40–57, doi:10.2113/gsjfr.44.1.40.

Huber, B.T., Petrizzo, M.R., Watkins, D.K., Haynes, S.J., MacLeod, K.G., 2016, Correlation of Turonian continental margin and deep-sea sequences in the subtropical Indian Ocean sediments by integrated planktonic foraminiferal and calcareous nannofossil biostratigraphy: Newsletters on Stratigraphy (in press).

Jarvis, I., Gale, A.S., Jenkyns, H.C., and Pearce, M.A., 2006, Secular variation in Late Cretaceous carbon isotopes: A new $\delta^{13}C$ carbonate reference curve for the Cenomanian–Campanian (99.6–70.6 Ma): Geological Magazine, v. 143, no. 5, p. 561–608, doi:10.1017/S0016756806002421.

Jarvis, I., Lignum, J.S., Gröcke, D.R., Jenkyns, H.C., and Pearce, M.A., 2011, Black shale deposition, atmospheric CO_2 drawdown, and cooling during the Cenomanian–Turonian ocean anoxic event: Paleoceanography, v. 26, p. PA3201, doi:10.1029/2010PA002081.

Jeng, W.-L., 2006, Higher plant *n*-alkane average chain length as an indicator of petrogenic hydrocarbon contamination in marine sediments: Marine Chemistry, v. 102, p. 242–251.

Jiménez Berrocoso, Á., MacLeod, K.G., Huber, B.T., Lees, J.A., Wendler, I., Bown, P.R., Mweneinda, A.K., Isaza Londono, C., and Singano, J.M., 2010, Lithostratigraphy, biostratigraphy and chemostratigraphy of Upper Cretaceous sediments from southern Tanzania: Tanzania Drilling Project Sites 21–26: Journal of African Earth Sciences, v. 57, p. 47–69, doi:10.1016/j.jafrearsci.2009.07.010.

Jiménez Berrocoso, Á., Huber, B.T., MacLeod, K.G., Petrizzo, M.R., Lees, J.A., Wendler, I., Coxall, H., Mweneinda, A.K., Falzoni, F., Birch, H., Singano, J.M., Haynes, S., Cotton, L., Wendler, J., Bown, P.R., Robinson, S.A., and Gould, J., 2012, Lithostratigraphy, biostratigraphy and chemostratigraphy of Upper Cretaceous and Paleogene sediments from southern Tanzania: Tanzania Drilling Project Sites 27–35: Journal of African Earth Sciences, v. 70, p. 36–57, doi:10.1016/j.jafrearsci.2012.05.006.

Jiménez Berrocoso, Á., Huber, B.T., MacLeod, K.G., Petrizzo, M.R., Lees, J.A., Wendler, I., Coxall, H., Mweneinda, A.K., Falzoni, F., Birch, H., Haynes, S.J., Bown, P.R., Robinson, S.A., and Singano, J.M., 2015, The Lindi Formation (Upper Albian–Coniacian) and Tanzania Drilling Project Sites 36–40 (Lower Cretaceous to Paleogene): Lithostratigraphy, biostratigraphy and chemostratigraphy: Journal of African Earth Sciences, v. 101, p. 282–308, doi:10.1016/j.jafrearsci.2014.09.017.

John, E.H., Pearson, P.N., Coxall, H.K., Birch, H., Wade, B.S., and Foster, G.L., 2013, Warm ocean processes and carbon cycling in the Eocene: Philosophical Transactions of the Royal Society (London), ser. A, v. 371, p. 1–20, doi:10.1098/rsta.2013.0099.

Johnston, D., Farquhar, J., and Canfield, D., 2007, Sulfur isotope insights into microbial sulfate reduction: When microbes meet models: Geochimica et Cosmochimica Acta, v. 71, p. 3929–3947, doi:10.1016/j.gca.2007.05.008.

Kasten, S., and Jørgensen, B.B., 2000, Sulfate reduction in marine sediments, *in* Schulz, H.D., and Zebel, M., eds., Marine Geochemistry: Berlin, Springer p. 263–281, doi:10.1007/978-3-662-04242-7_8.

Killops, S., and Killops, V., 2005, Introduction to Organic Geochemistry, Volume 2: Malden, Massachusetts, Blackwell Science Ltd., 393 p.

Kürschner, W.M., Batenburg, S.J., and Mander, L., 2013, Aberrant *Classopollis* pollen reveals evidence for unreduced (2*n*) pollen in the conifer family Cheirolepidiaceae during the Triassic-Jurassic transition: Proceedings, Biological Sciences, v. 280, no. 20131708, p. 1–8, doi:10.1098/rspb.2013.1708.

Leavitt, W.D., Halevy, I., Bradley, A.S., and Johnston, D.T., 2013, Influence of sulfate reduction rates on the Phanerozoic sulfur isotope record: Proceedings of the National Academy of Sciences of the United States of America, v. 110, p. 11,244–11,249, doi:10.1073/pnas.1218874110.

Leckie, R.M., 1987, Paleoecology of mid-Cretaceous planktonic foraminifera: A comparison of open ocean and

epicontinental sea assemblages: Micropaleontology, v. 33, p. 164–176, doi:10.2307/1485491.

Lees, J.A., 2007, New and rarely reported calcareous nannofossil from the Late Cretaceous of coastal Tanzania: Outcrop samples and Tanzania Drilling Project Sites 5, 9 and 15: Journal of Nannoplankton Research, v. 29, no. 1, p. 39–65.

Lees, J.A., and Bown, P.R., 2016, New and intriguing calcareous nannofossils from the Turonian (Upper Cretaceous) of Tanzania: Journal of Nannoplankton Research, v. 36, no. 1, p. 83–95.

Lehmann, R., 1963, Étude des Globotruncanidés du Crétacé supérieur de la province de Tarfaya (Maroc occidental): Notes du Service Géologique du Maroc, v. 21, p. 133–179.

Li, J., Peng, J., and Batten, D.J., 2015, Palynomorph assemblages from the Fenghoushan Group, southern Qinghai, China: Their age and palaeoenvironmental significance: Science Bulletin v. 60, no. 4, p. 470–476, doi:10.1007/s11434-014-0677-8.

Loeblich, A.R., and Tappan, H., 1961, The genera *Microaulopora* Kuntz, 1895, and *Guembelina* Kuntz, 1895, and the status of *Guembelina* Egger, 1899: Journal of Paleontology, v. 35, p. 625–627.

Lowenstein, T.K., Hardie, L.A., Timofeeff, M.N., and Demicco, R.V., 2003, Secular variation in seawater chemistry and the origin of calcium chloride basinal brines: Geology, v. 31, p. 857–860, doi:10.1130/G19728R.1.

MacLeod, K.G., Huber, B.T., Jiménez Berrocoso, Á., and Wendler, I., 2013, A stable and hot Turonian without glacial $\delta^{18}O$ excursions is indicated by exquisitely preserved Tanzanian foraminifera: Geology, v. 41, no. 10, p. 1083–1086, doi:10.1130/G34510.1.

Marie, P., 1941, Les foraminifères de la craie a *Belemnitella mucronata* du Bassin de Paris: Mémoires du Muséum National d'Histoire Naturelle, v. 12, p. 237–258.

Marynowski, L., Zatoń, M., Simoneit, B.R.T., Otto, A., Jędrysek, M.O., Grelowski, C., and Kurkiewicz, S., 2007, Compositions, sources and depositional environments of organic matter from Middle Jurassic clays of Poland: Applied Geochemistry, v. 22, p. 2456–2485, doi:10.1016/j.apgeochem.2007.06.015.

McConnaughey, T., 1989a, ^{13}C and ^{18}O isotopic disequilibrium in biological carbonates: I. Patterns: Geochimica et Cosmochimica Acta, v. 53, p. 151–162.

McConnaughey, T., 1989b, ^{13}C and ^{18}O isotopic disequilibrium in biological carbonates: II. *In vitro* simulation of kinetic isotope effects: Geochimica et Cosmochimica Acta, v. 53, p. 163–171, doi:10.1016/0016-7037(89)90283-4.

McFadden, K.A., and Kelly, A.E., 2011, Carbon and sulfur stable isotopic systems and their application in paleoenvironmental analysis, *in* Dornbos, S., LaFlamme, M., and Schiffbauer, J.D., eds., Topics in Geobiology: Quantifying the Evolution of Early Life: Berlin, Springer, p. 403–450, doi:10.1007/978-94-007-0680-4_15.

Meister, P., 2013, Two opposing effects of sulfate reduction on carbonate precipitation in normal marine, hypersaline, and alkaline environments: Geology, v. 41, p. 499–502, doi:10.1130/G34185.1.

Meyer, S.E., 1995, Ephedra: Provo, Utah, U.S. Department of Agriculture Forest Service, Rocky Mountain Research Station.

Moore, T.S., Murray, R.W., Kurtz, A.C., and Schrag, D.P., 2004, Anaerobic methane oxidation and the formation of dolomite: Earth and Planetary Science Letters, v. 229, p. 141–154, doi:10.1016/j.epsl.2004.10.015.

Ogg, J., and Gradstein, F.M., 2015, Time Scale Creator version 6.2: https://engineering.purdue.edu/Stratigraphy/tscreator/index/index.php (last accessed 12 August 2016).

Pearson, P.N., and Coxall, H.K., 2014, Origin of the Eocene planktonic foraminifer *Hantkenina* by gradual evolution: Palaeontology, v. 57, no. 2, p. 243–267, doi:10.1111/pala.12064.

Pearson, P.N., Ditchfield, P.W., Singano, J., Harcourt-Brown, K.G., Nicholas, C.J., Olsson, R.K., Shackleton, N.J., and Hall, M.A., 2001, Warm tropical sea surface temperatures in the Late Cretaceous and Eocene Epochs: Nature, v. 413, p. 481–487, doi:10.1038/35097000.

Pearson, P.N., Nicholas, C.J., Singano, J.M., Bown, P.R., Coxall, H.K., van Dongen, B.E., Huber, B.T., Karega, A., Lees, J.A., Msaky, E., Pancost, R.D., Pearson, M., and Roberts, A.P., 2004, Paleogene and Cretaceous sediment cores from the Kilwa and Lindi areas of coastal Tanzania Drilling Project Sites 1–5: Journal of African Earth Sciences, v. 39, p. 25–62, doi:10.1016/j.jafrearsci.2004.05.001.

Perch-Nielsen, K., 1985, Mesozoic calcareous nannofossils, *in* Bolli, H.M., Saunders, J.B., and Perch-Nielsen, K., eds., Plankton Stratigraphy: Cabridge ,Cambridge University Press, v. 1, p. 329–426.

Peryt, D., 1980, Planktic foraminifera zonation of the Upper Cretaceous in the middle Vistula River valley, Poland: Palaeontologia Polonica, v. 41, p. 3–101.

Pessagno, E.A., Jr., 1967, Upper Cretaceous planktonic foraminifera from the western Gulf Coastal Plain: Palaeontographica Americana, v. 5, no. 37, p. 243–445.

Peters, K.E., and Moldowan, J.M., 1993, The Biomarker Guide: Interpreting Molecular Fossils in Petroleum and Ancient Sediments: Englewood Cliffs, New Jersey, Prentice-Hall, 363 p.

Peters, K.E., Walters, C.C., and Moldowan, J.M., 2005, The Biomarker Guide: Volume 2. Biomarkers and Isotopes in Petroleum Exploration and Earth History (2nd ed.): Cambridge, UK, Cambridge University Press, p. 475–1155.

Petrizzo, M.R., 2000, Upper Turonian–Lower Campanian planktonic foraminifera from southern mid-high latitudes (Exmouth Plateau, NW Australia): Biostratigraphy and taxonomic notes: Cretaceous Research, v. 21, p. 479–505, doi:10.1006/cres.2000.0218.

Petrizzo, M.R., 2001, Late Cretaceous planktonic foraminifera from Kerguelen Plateau (ODP Leg 183): New data to improve the Southern Ocean biozonation: Cretaceous Research, v. 22, p. 829–855, doi:10.1006/cres.2001.0290.

Petrizzo, M.R., 2003, Late Cretaceous planktonic foraminiferal bioevents in the Tethys and in the Southern Ocean record: An overview: Journal of Foraminiferal Research, v. 33, p. 330–337, doi:10.2113/0330330.

Porthault, B., 1970, Le Sénonien inférieur de Puget-Théniers (Alpes-Maritimes) et sa microfaune, *in* Donze, P., Porthault, B., Thomel, G., and de Villoutreys, O., eds., Le Sénonien inférieur de Puget–Théniers (Alpes–Maritimes) et sa microfaune: Geobios, v. 3, p. 41–106, doi:10.1016/S0016-6995(70)80011-0.

Price, R.A., 1996, Systematics of the Gnetales: A review of morphological and molecular evidence: International Journal of Plant Sciences, v. 157, no. 6, supplement (Biology and Evolution of Gnetales), p. S40–S49.

Robinson, N., Eglinton, G., Brassell, S.C., and Cranwell, P., 1984, Dinoflagellate origin for sedimentary 4α-methylsteroids and 5α(H)-stanols: Nature, v. 308, p. 439–442, doi:10.1038/308439a0.

Rullkötter, J., Peakman, T.M., and ten Haven, H.L., 1994, Early diagenesis of terrigenous triterpenoids and its implications for petroleum geochemistry: Organic Geochemistry, v. 21, no. 3–4, p. 215–233, doi:10.1016/0146-6380(94)90186-4.

Scalan, R.S., Smith, J.S., 1970, An improved measure of the odd-even predominance in the normal alkanes of sediment extracts and petroleum: Geochimica et Cosmochimica Acta, v. 34, p. 611–620.

Scheibnerová, V., 1962, Upper Cretaceous, middle Turonian—Klippen belt of West Carpathians in Slovakia, Czechoslovakia: Slovenska Akademia Vied, Bratislava: Geologických Sborník, v. 13, p. 225.

Schrag, D.P., Higgins, J.A., MacDonald, F.A., and Johnston, D.T., 2013, Authigenic carbonate and the history of the global carbon cycle: Science, v. 339, p. 540–543, doi:10.1126/science.1229578.

Schrank, E., 2010, Pollen and spores from the Tendaguru Beds, Upper Jurassic and Lower Cretaceous of southeast Tanzania: Palynostratigraphical and paleoecological implications: Palynology, v. 34, no. 1, p. 3–42, doi:10.1080/01916121003620106.

Spero, H.J., 1992, Do planktic foraminifera accurately record shifts in the carbon isotopic composition of seawater ΣCO_2?: Marine Micropaleontology, v. 19, no. 4, p. 275–285, doi:10.1016/0377-8398(92)90033-G.

Srivastava, S.K., 1976, The fossil pollen genus *Classopollis*: Lethaia (Oslo), v. 9, p. 437–457.

Sweet, A.R., and McIntyre, D.J., 1988, Late Turonian marine and nonmarine palynomorphs from the Cardium Formation, north central Alberta Foothills, Canada, *in* James, D.P., and Leckie, D.A., eds., Sequences, Stratigraphy, Sedimentology: Surface and Subsurface: Canadian Society of Petroleum Geologists Memoir 15, p. 499–516.

Trujillo, E.F., 1960, Upper Cretaceous foraminifera from near Redding, Shasta County, CA: Journal of Paleontology, v. 34, p. 290–346.

van Dongen, B.E., Talbot, H.M., Schouten, S., Pearson, P.N., and Pancost, R.D., 2006, Well preserved Palaeogene and Cretaceous biomarkers from the Kilwa area, Tanzania: Organic Geochemistry, v. 37, p. 539–557, doi:10.1016/j.orggeochem.2006.01.003.

Verbeek, J., 1977, Calcareous Nannoplankton Biostratigraphy of Middle and Upper Cretaceous Deposits in Tunisia, Southern Spain, and France: Utrecht Micropaleontological Bulletin 16, 158 p.

Volkman, J.K., 1986, A review of sterol markers for marine and terrigenous organic matter: Organic Geochemistry, v. 9, no. 2, p. 83–99, doi:10.1016/0146-6380(86)90089-6.

Volkman, J.K., Gillan, F.T., and Johns, R.B., 1981, Sources of neutral lipids in a temperate intertidal sediment: Geochimica et Cosmochimica Acta, v. 45, p. 1817–1828, doi:10.1016/0016-7037(81)90012-0.

Volkman, J.K., Kearney, P., and Jeffery, S.W., 1990, A new source of 4-methyl sterols and 5α(H)-stanols in sediments: Prymnesiophyte microalgae of the genus *Pavlova*: Organic Geochemistry, v. 15, no. 5, p. 489–497, doi:10.1016/0146-6380(90)90094-G.

Volkman, J.K., Zhang, Z., Xie, X., Qin, J., and Borjigin, T., 2015, Biomarker evidence for *Botryococcus* and methane cycle in the Eocene Huadian oil shale, NE China: Organic Geochemistry, v. 78, p. 121–134, doi:10.1016/j.orggeochem.2014.11.002.

Wendler, J., and Bown, P., 2013, Exceptionally well-preserved Cretaceous microfossils reveal new biomineralization styles: Nature Communications, v. 4, p. 2052, doi:10.1038/ncomms3052.

Wendler, I., Huber, B.T., MacLeod, K.G., and Wendler, J., 2011, Early evolutionary history of *Tubulogenerina* and *Colomia*, with new species from the Turonian of East Africa: Journal of Foraminiferal Research, v. 41, no. 4, p. 384–400, doi:10.2113/gsjfr.41.4.384.

Wendler, I., Huber, B.T., MacLeod, K.G., and Wendler, J., 2013, Stable oxygen and carbon isotope systematics of exquisitely preserved Turonian foraminifera from Tanzania—Understanding isotopic signatures: Marine Micropaleontology, v. 102, p. 1–33, doi:10.1016/j.marmicro.2013.04.003.

Wendler, I., Wendler, J.E., and Clarke, L.J., 2016, Sea-level reconstruction for Turonian sediments from Tanzania based on integration of sedimentology, microfacies, geochemistry and micropaleontology: Palaeogeography, Palaeoclimatology, Palaeoecology, v. 441, p. 528–564, doi:10.1016/j.palaeo.2015.08.013.

Wilson, P.A., and Roberts, H.H., 1995, Density cascading: Off-shelf sediment transport, evidence and implications, Bahama Banks: Journal of Sedimentary Research, v. A65, no. 1, p. 45–56.

Zhelezinskaia, I., Kaufman, A.J., Farquhar, J., and Cliff, J., 2014, Large sulfur isotope fractionations associated with Neoarchean microbial sulfate reduction: Science, v. 346, p. 742–744, doi:10.1126/science.1256211.

Science Editor: David I. Schofield
Associate Editor: Thomas Olszewski

Manuscript Received 25 September 2015
Revised Manuscript Received 10 June 2016
Manuscript Accepted 20 October 2016

Printed in the USA